CAVITY FLOW PAST AN OBSTACLE INCLUDING GRAVITY EFFECTS

by

Chao-yung Ou

Dissertation submitted to the Graduate Faculty of the
Virginia Polytechnic Institute and State University
in partial fulfillment of the requirements for the degree of

DOCTOR OF PHILOSOPHY

in

Civil Engineering

APPROVED:

D. N. Contractor

J. M. Wiggert

R. M. Barker

D. T. Mook

C. B. Ling

Blacksburg, Virginia

ACKNOWLEDGEMENTS

The author wishes to express his sincere gratitude to his advisor Professor D. N. Contractor. Without his instruction and encouragement this thesis could never have been written.

Professors J. M. Wiggert, R. M. Barker, C. B. Ling and D. T. Mook are gratefully acknowledged for serving on the author's doctoral committee and for their helpful suggestions and direction from time to time.

Acknowledgements are extended to the Department of Civil Engineering, Virginia Polytechnic Institute and State University, for the financial support given during the author's graduate program. Thanks are also due to the computer center of VPI&SU and EBASCO SERVICES for providing the computer service.

TABLE OF CONTENTS

CHAPTER I

INTRODUCTION

1.1 Preface

The purpose of this study is to obtain numerical solutions of cavity flow past a two-dimensional roughness element in an open channel with gravity effects included. For a long time, the use of large roughness elements in steep channels to increase resistance to flow or the use of baffle blocks in still basins to dissipate energy has been found useful. Because of its practical importance for the design of hydraulic structures and because this fascinating and complex phenomenon lends itself to theoretical analysis, it has continuously attracted the attention of many investigators (1). Many experimental studies have been conducted in the past, and the results show that the effectiveness of energy dissipation by use of large elements depends on the ratio of element height to element spacing. In other words, energy dissipation depends on the mutual interference of cavities or wakes formed behind the elements. A few empirical equations have been presented for design purposes. However, theoretical simulation and interpretation have not progressed too far. Even though cavity flow is an important and extensively studied part of hydrodynamics, most of the attention has been focused on the prediction of cavity drag force rather than the prediction of the relation between cavity length, element height and flow parameters. It is the aim of this study to find such a relation.

An assumption frequently used in solving cavity flow problems is derived from the so-called "free-streamline theory" which states that a free streamline is a line of constant stream function along which the velocity and pressure are constant and which separates the flow field into regions of different energy. On the basis of this assumption the complex cavity flow problems are turned into a relatively simple mixed boundary value problems. The Dirichlet condition will hold over the fixed boundaries of the flow, where as the Neumann condition will hold over the free stream line. The analysis of free stream line flow, then, can proceed with the aid of the hodograph or the logarithmic hodograph and the Schwarz-Christoffel transformation. However, when the gravitational effect is significant, the assumption of constant velocity is no longer valid, since the velocity has to change with elevation, even though the pressure is still a constant. And the analytic solution of this problem becomes extremely difficult if not impossible. Therefore, numerical solutions become necessary.

1.2 Method of Solution-Relaxation Method

A well-known method which speeds up numerical solutions with simple iteration is the so-called relaxation method. This method was first employed by Gauss in 1823 and later on was greatly extended and applied by Southwell (2) in the 1940's. Any method in which a new approximation is obtained from the previous approximation and its residue may be called a relaxation method. The central idea of this method is to use the residue as an indicator of the correction

to be made for the new approximation. The advantage of using the relaxation technique lies in the fact that the numerical process is simple and straightforward, yet it can be used to obtain solutions for a wide variety of problems which cannot be solved by standard methods. For instance, partial differential equations such as the Laplace, the Poisson and the biharmonic equations are often encountered in engineering practice and numerous general solutions have been obtained for simple boundary conditions. But, when the boundary conditions are complex, general solutions are usually unobtainable and the relaxation method becomes particularly valuable since a complex boundary condition can be handled almost as easily as a simple one. In the past the resolution of any significant problem by the relaxation method would have required extensive hand computation and would have been very time-consuming. However, the advent of the digital computer has completely eliminated such difficulty and made the method extremely powerful.

1.3 Basic Assumptions

In natural open channels, two dimensional uniform steady flow seldom exists. The flow and resistance change from time to time and vary from place to place. The analysis of cavity flow is so complex that the solution of three dimensional flows is practically impossible. In order to simplify the solution and still not lose its practical value, the following assumptions are made:

(1) The flow is two-dimensional, uniform, and steady, and no energy loss occurs throughout the flow field.

(2) The pressure within the cavity is constant and equal to the pressure that exists in the uniform steady flow region. Thus by applying Bernoulli's equation to point (1) and (2) (See Figure 1)

$$h_1 + Z_1 + \frac{V_1^2}{2g} = \frac{P_c}{\gamma} + Z_2 + \frac{V_2^2}{2g}$$

$$\therefore \quad \frac{P_c}{\gamma} = h_1$$

in which h is the water depth, v is the flow velocity, z is the channel elevation, γ is the unit weight of fluid and g is the acceleration due to gravity.

(3) No vorticity exists within the flow region, i.e., the flow is irrotational.

(4) No hydraulic jump is assumed to occur within the flow field, since the hydraulic jump would disrupt the continuity of the free surface and cause energy losses. Therefore, the flow will be, at most, in incipient jump conditions. Based on the above assumptions, the complex cavity flow problem in this study can be idealized as a two dimensional potential flow problem which can be represented by the well known Laplace equation.

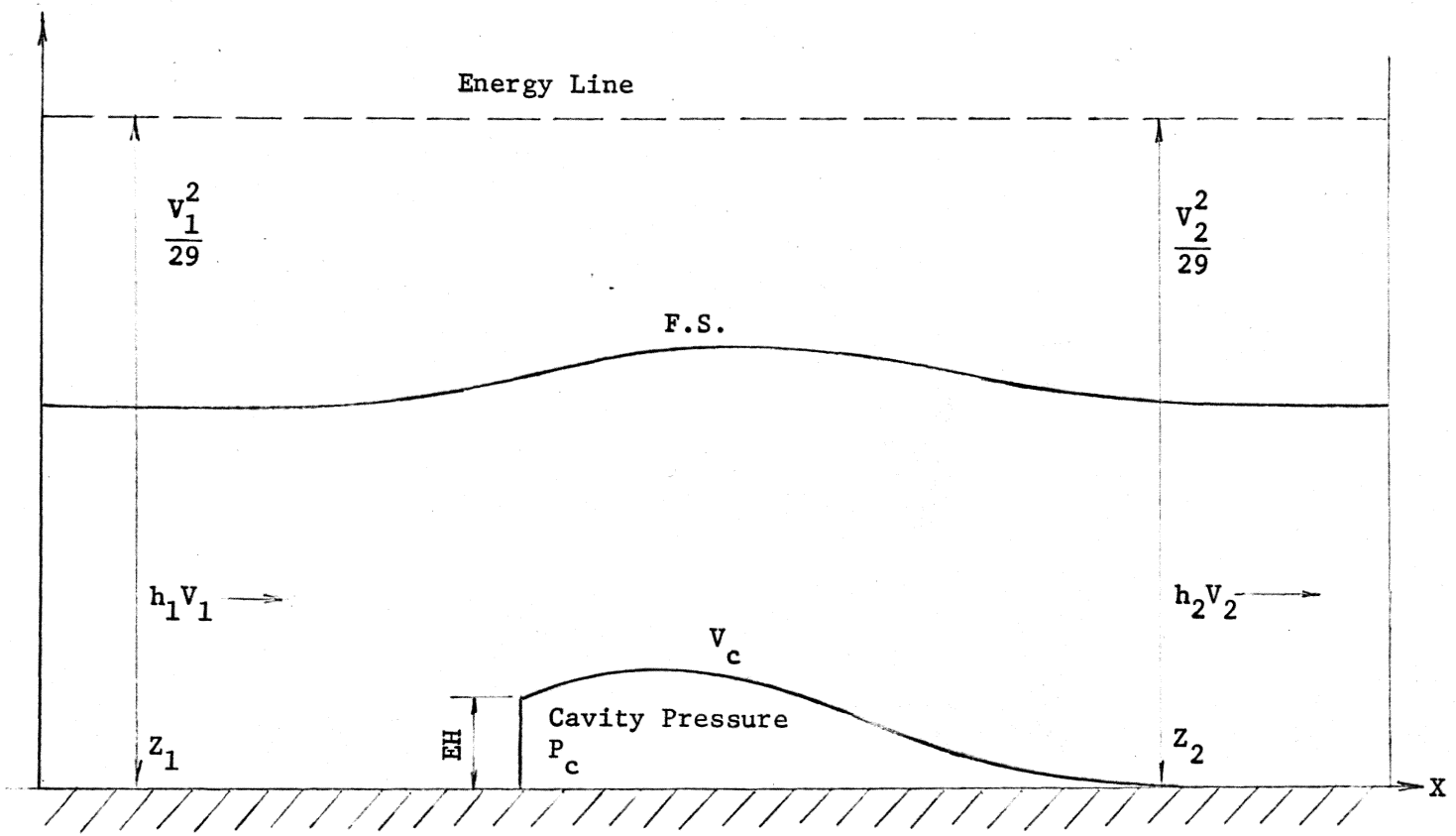

Figure 1 Two Dimensional Flow Past an Obstacle

CHAPTER II

LITERATURE REVIEW

2.1 Early History of Free Streamline Analysis

The analysis of cavity flow started early in the nineteenth century. Helmholtz in 1868 first introduced his well-known free streamline theory to solve discontinuous flow problems which initiated an important era of ideal fluid analysis and resulted in the solution of simple cavity flow problems. His solution of the flow into a Borda mouthpiece is representative of his method of solution to free jet problems (3). G. Kirchhoff in the following year analyzed the flow from a plane orifice and that past a normal plate. His method is basically an enlargement and extension of Helmholtz's solution to jet problems. Lord Rayleigh (1876) extended the free streamline analysis to the case of flow past an inclined plate and calculated the plane-orifice coefficients for Kirchhoff's solution. Max Planck in 1884 introduced the logarithmic hodograph for the solution of free-streamline problems. In 1890, a major step in the analysis of free-streamline problems was made by J. H. Michell and N. E. Joukowsky. Michell initiated the use of the Schwarz-Christoffel transformation to link the auxiliary t plane with the logarithmic hydograph and complex potential plane. This is the essence of the direct, analytic approach to the free streamline problem. By the direct method, the applicability of the free streamline analysis technique was much enlarged. Joukowsky, on the contrary, greatly

extended the use of an indirect method introduced by Planck. He recreated the solutions of all the specific problems treated by his predecessors and solved many new problems which has presented difficulties when their solution was attempted by the Kirchhoff method.

In the early part of this century, two new considerations appeared: T. Levi-Civita (1901) suggested that free streamlines could start from rounded bodies as well as from sharp-cornered ones, and D. Riabouchinsky in 1919 (and Joukowsky in 1890) introduced the new idea that the velocity along free streamlines could be permitted to exceed that of the approaching stream. This permitted the obtaining of more realistic body drags than found by Kirchhoff and his successors. There were still many other contributions to the free streamline analysis not mentioned here. Those were H. Lamb (1879), A. B. Bassit (1888), A. E. H. Love (1891), M. Rethy (1894), A. G. Greenhill (1910), R. Von Mises (1917), A. Betz and E. Petersohn (1931). All of their contributions have been outlined briefly in reference (3).

2.2 Free Streamline and Relaxation Method

In the mid 1940's, a new approach to the solution of free streamline problems was first developed by Southwell. Southwell and his associate Vaisey in 1945, applied the relaxation technique to solve free streamline flow problems, such as the flow through a Borda mouthpiece, orifice plate in a pipe, wake behind a circular

cylinder. By his method, the earlier complex mapping technique was replaced by a simple iterative process, which enabled the solution of diverse practical problems. A more significant contribution of his work is that the gravitational effect can be easily taken into account without extra manipulation. Two typical examples of their free surface analysis were "Flow under gravity through an orifice plate" and "Flow at a free overfall".

In 1953, McNown, Hsu, and Yih (4) reviewed the application of the relaxation method in fluid flow problems. In addition to the detailed review of the relaxation technique in the Z plane (x and y) they suggested that for some problems, it was preferable to apply the relaxation technique in the $\bar{W}$ plane ($\phi \sim \psi$). Because the region of interest in fluid flow can always be bounded by a pair of equipotential lines and streamlines, no irregular star (in the finite difference mesh) will be encountered. The practical value of the method has been illustrated well by the application of the method to solve a variety of problems including flow through boundary transitions, flow with a free surface, and seepage problems. They solved the following problems:

(1) flow with cavitation about a head form,

(2) flow through a two dimensional inlet transition between a reservoir and conduit,

(3) flow over a high weir,

(4) impingement of a jet on a flat plate and

(5) seepage through a vertical wall.

In 1961, Garrett Birkhoff (5) gave a survey of methods for computing three classes of potential flows with free streamlines:

(1) plane flows having free boundaries and curved fixed boundaries without gravity.

(2) plane flow having free boundaries and straight fixed boundaries with gravity and

(3) axially symmetric flow having free boundaries without gravity.

In his discussion about trial, free streamlines, he concluded that the relaxation method suffered from several defects: The shape of the free boundary was sensitive to small variations in the velocity, and it was hard to achieve accuracy near points of flow separation. Besides, it was tedious.

In response to Birkhoff's conclusion, Satya Prakash Garg (6) remarked that those who have worked with free streamlines notice that with a comparatively small adjustment of the boundary, the values of the velocity head Y_v changes by a much greater value. Thus the final solution is a sort of unstable equilibrium condition. To obtain a correct profile under such circumstances one has to work more or less intuitively, because a plot of the derived velocity head Y_v, gives only a rough qualitative indication concerning the change to be made in the ordinate Y of the profile. In view of this fact, Satya Prakash Garg suggested that if the process was reversed, computation of Y from an assumed distribution of Y_v should lead to a closer approximation. The application of the new values Y in place of Y_v would yield

a more satisfactory approximation. He applied the idea to analyse a two dimensional efflux with gravitational effects, and the result was found to be very satisfactory.

Markland in 1964 showed that the inverse function $x(\phi,\psi)$ and $y(\phi,\psi)$ might be used to solve potential flow problems and that the solution can be obtained in a more direct manner if the proper inverse functions are selected for the problems at hand. In his solution of "Flow at a free overfall", Markland normalized the physical plane and then mapped it into the complex plane (W-plane) where the relaxation process was performed. The mesh size used in his study was a = 1.0 and 1/2 in turn for Froude numbers F = 1, 2, 4, and 8 with a = 1/4 for F = 1 only. The results were then compared with the experimental work presented by Rouse. It was found satisfactory.

Using the same approach as Markland did Jeppson (8) in 1966 also successfully solved a number of plane and axisymmetric cavity flow problems. His work mainly dealt with problems of seepage through porous media and dealt with some problems of jet and cavity flow.

The latest development in free streamline analysis by a relaxation method could be represented by Mogel and Street (9) (1972). Mogel and Street developed a numerical method for steady state cavity flows that provided a systematic correction of an initial assumed free streamline position. The method developed was based on an inviscid, irrotational and incompressible flowfield, used a numerical finite difference representation with the fluid velocity as a

dependent variable, and obtained a solution by successive-over-relaxation. The key feature of the method is that the Riabouchinsky model was employed and the numerical solution was obtained in the physical plane. No gravity effects were included in their study.

2.3 Flow Over a Sill

In early 1960, a different approach in free streamline analysis with gravitational effects appeared in connection with the design of an end sill for energy dissipation in stilling basins. G. Z. Watters and Robert L. Street (10) in 1964 developed a general theory for two dimensional flow over sills by means of complex function theory and conformal mapping. The theory enables one to calculate the velocity and pressure at any point in the flow as well as the location of the free surface for an arbitrary local change in the channel bottom. The theory is first developed for flow over a simple vertical step in the channel bottom and then broadened to apply to the flow over a polygonal sill in the channel, and finally it is extended to flow over a smooth sill. However, no cavity or wake behind the sill is taken into account.

A most up-to-date and valuable development in cavity flow analysis with gravitational effect is seen in the paper "Supercritical Flow Over Sills at Incipient Jump Conditions" by K. S. Karki, A. Chander, and R. C. Malhotra (11) in 1972. Based on experimental observation, they made the following assumptions for their analytical study:

(1) The pressure head on the upstream face of the sill is uniform and is equal to $Z + d_c$ (see Figure 2).

(2) The flow depth at the section of maximum water rise is equal to the critical depth for the given discharge.

(3) The pressure head at the top of the downstream face of the sill is $d_c - Z$, and varied hydrostatically towards the bottom. Thus, the pressure head at the bottom of the downstream face is d_c.

With the above assumptions and applying the momentum and Bernoulli's equations, they obtained equations for calculating the required sill height that would produce incipient hydraulic jump flow conditions, and maximum water depth.

$$\frac{Z}{d_1} = \frac{1}{2}\frac{d_c}{d_1}\left\{-1 + \sqrt{1+4\left[\frac{d_c}{d_1} + 0.5\left(\frac{d_1}{d_c}\right)^2 - 1.5\right]}\right\}$$

$$\frac{d_{max}}{d_c} = \frac{d_1}{d_c} + 0.5\,\frac{d_c}{d_1} - 0.5$$

where Z is the sill height as shown in Figure 2.

Some specific conclusions reached were:

(1) The flow depth at the point of maximum water rise is approximately equal to the critical depth.

(2) The water jet separates from the boundary at a distance equal to 1 to 1 1/4 times the height of the sill ahead of its upstream face. It then reattaches to the boundary at a distance equal to six to seven times the height of the sill downstream of its upstream face. The point of maximum water rise occurs at a distance equal to three to four times the sill height from the upstream face.

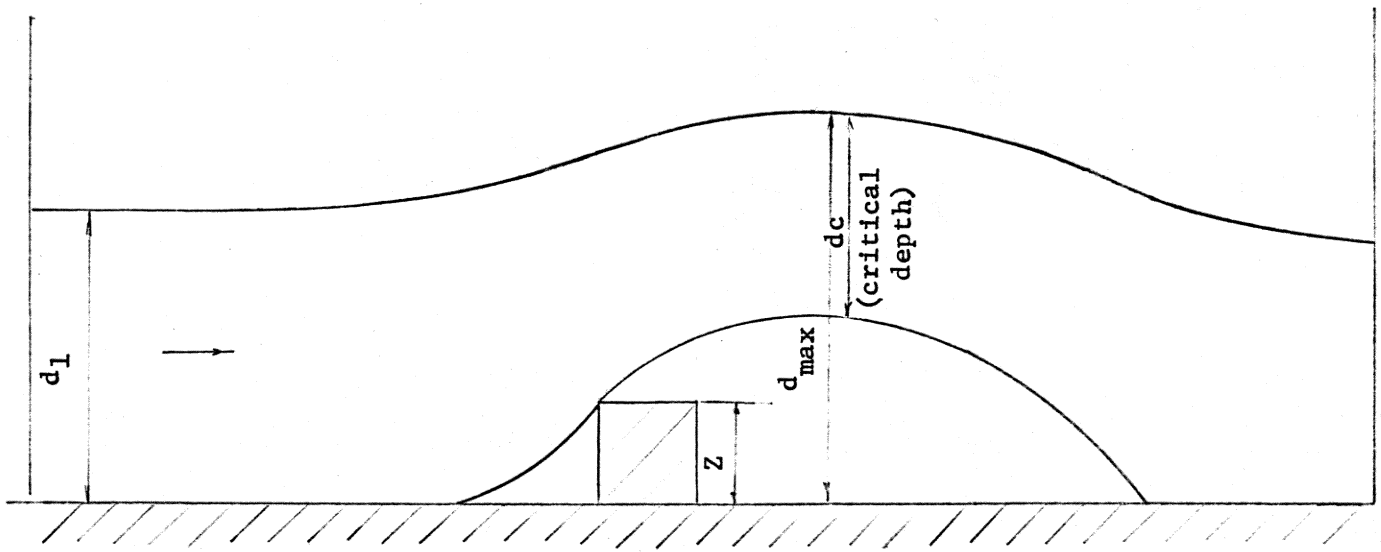

Figure 2 Flow Over the Sill

CHAPTER III

FINITE DIFFERENCE WITH RELAXATION METHOD

3.1 General Description

Finite-difference formulations have been used for many years. The theory and application of the method are given in texts of numerical analysis (12). When using finite differences with the relaxation technique to solve the Laplace equation, a network of grid points is first established throughout the region of interest. Then at every grid point, approximate initial values of the stream function ψ (or velocity potential ϕ) are assigned. Finally successive refinements of these values are made according to finite difference formulas representing the Laplace equation and boundary conditions. A general relaxation pattern of square grid with irregular stars has been derived by Streeter (13). Consider a star as shown in Figure 3b. By Taylor's expansion, one has, up to terms of the second degree in Δa, the following relations:

$$\psi_1 = \psi_o - \psi_x \lambda_1 a + \psi_{xx} \frac{\lambda_1^2 a^2}{2} \tag{3.1}$$

$$\psi_2 = \psi_o + \psi_x \lambda_2 a + \psi_{xx} \frac{\lambda_2^2 a^2}{2} \tag{3.2}$$

$$\psi_3 = \psi_o - \psi_y \lambda_3 a + \psi_{yy} \frac{\lambda_3^2 a^2}{2} \tag{3.3}$$

$$\psi_4 = \psi_o + \psi_y \lambda_4 a + \psi_{yy} \frac{\lambda_4^2 a^2}{2} \tag{3.4}$$

Eliminating ψ_x from the first two formulas

$$\lambda_2\psi_1 + \lambda_1\psi_2 - (\lambda_1 + \lambda_2)\psi_o = \frac{a^2}{2}\lambda_1\lambda_2(\lambda_1 + \lambda_2)\psi_{xx} \quad .$$

Similarly,

$$\lambda_4\psi_3 + \lambda_3\psi_4 - (\lambda_3 + \lambda_4)\psi_o = \frac{a^2}{2}\lambda_3\lambda_4(\lambda_3 + \lambda_4)\psi_{yy} \quad .$$

Thus the Laplace equation $\psi_{xx} + \psi_{yy} = 0$ becomes

$$\frac{\psi_1}{\lambda_1(\lambda_1 + \lambda_2)} + \frac{\psi_2}{\lambda_2(\lambda_1 + \lambda_2)} + \frac{\psi_3}{\lambda_3(\lambda_3 + \lambda_4)} + \frac{\psi_4}{\lambda_4(\lambda_3 + \lambda_4)} -$$

$$\left(\frac{1}{\lambda_1\lambda_2} + \frac{1}{\lambda_3\lambda_4}\right)\psi_o = 0$$

After multiplication by $\frac{\lambda_1\lambda_2\lambda_3\lambda_4}{\lambda_1\lambda_2 + \lambda_3\lambda_4}$, the equation again becomes

$$R_o = D_1\psi_1 + D_2\psi_2 + D_3\psi_3 + D_4\psi_4 - \psi_o = 0 \qquad (3.5)$$

in which

$$D_1 = \frac{\lambda_2\lambda_3\lambda_4}{(\lambda_1\lambda_2 + \lambda_3\lambda_4)(\lambda_1 + \lambda_2)}, \quad D_2 = \frac{\lambda_1\lambda_3\lambda_4}{(\lambda_1\lambda_2 + \lambda_3\lambda_4)(\lambda_1 + \lambda_2)}$$

$$D_3 = \frac{\lambda_1\lambda_2\lambda_4}{(\lambda_1\lambda_2 + \lambda_3\lambda_4)(\lambda_3 + \lambda_4)}, \quad D_4 = \frac{\lambda_1\lambda_2\lambda_3}{(\lambda_1\lambda_2 + \lambda_3\lambda_4)(\lambda_3 + \lambda_4)}$$

The R_0 is called residue. At a regular star (4 equal strings) λ_1, λ_2, λ_3, λ_4 are all equal to 1. Then $D_1 = D_2 = D_3 = D_4 = 1/4$, and Laplace equation at a regular star becomes

$$R_o = \psi_1 + \psi_2 + \psi_3 + \psi_4 - 4\psi_o = 0 \qquad (3.6)$$

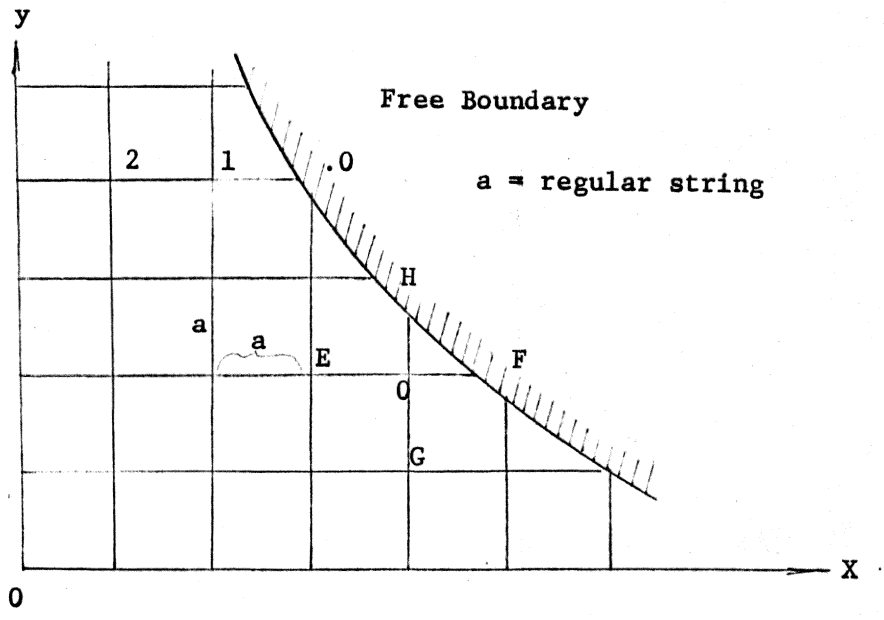

(a)

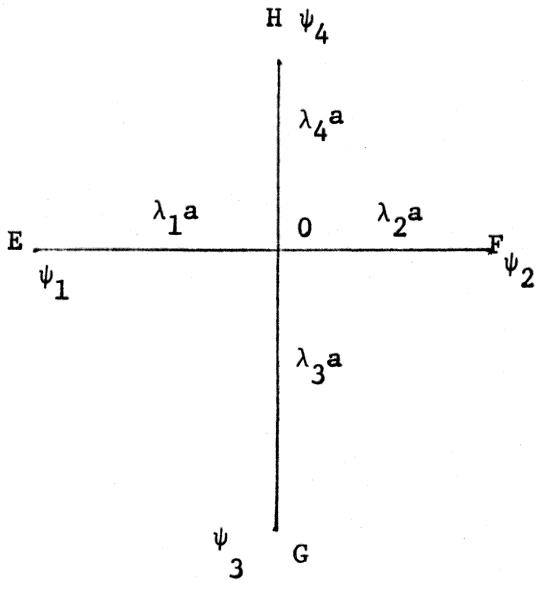

(b)

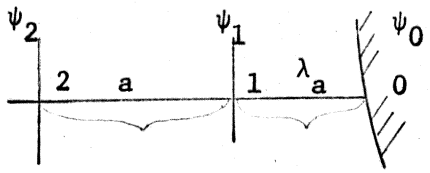

(c)

Figure 3 Flow Field with Irregular Strings

To satisfy the boundary condition along the free boundary, the derivative ($\frac{\partial\psi}{\partial n} = \frac{\psi_o - \psi_1}{\Delta n}$) at the boundary also has to be evaluated. Even though the assumption of local linearity approaches the actual condition, better results can be obtained by the finite difference formula for the derivative based on three ψ-values as shown in Figure 3c. Again by the Taylor expansion,

$$\psi_o = \psi_1 + \lambda a\psi_x + \psi_{xx}\frac{\lambda^2 a^2}{2} + \ldots \tag{3.7}$$

$$\psi_o = \psi_2 + (a + \lambda a)\psi_x + \psi_{xx}\frac{(a+\lambda a)^2}{2} + \ldots \tag{3.8}$$

Multiplying (3.7) by $\frac{(a+\lambda a)^2}{2}$, (3.8) by $\frac{(\lambda a)^2}{2}$ and subtracting (3.7) from (3.8)

$$\frac{(\lambda a)^2}{2}\psi_o - \frac{(\lambda a+a)^2}{2}\psi_o = \frac{(\lambda a)^2}{2}\psi_2 - \frac{(\lambda a+a)^2}{2}\psi_1 + [\lambda a - (\lambda a+a)]\frac{(\lambda a)(\lambda a+a)}{2}\psi_x$$

$$(\psi_1-\psi_o)(\lambda a+a)^2 - (\psi_2-\psi_o)(\lambda a)^2 = \lambda a(\lambda a+a)(-a)\,\psi_x$$

$$\frac{(\psi_1-\psi_o)(\lambda a+a)}{\lambda a^2} - \frac{(\psi_2-\psi_o)\lambda a}{a(\lambda a+a)} = -\psi_x$$

or

$$\psi_x = -\frac{(\psi_1-\psi_o)}{\lambda a}(1+\lambda) + \frac{(\psi_2-\psi_o)\lambda}{a(1+\lambda)}$$

$$= \frac{\psi_o - \psi_1}{a}\left(1 + \frac{1}{\lambda}\right) - \frac{(\psi_o - \psi_2)}{a}\,\frac{1}{\left(1 + \frac{1}{\lambda}\right)}$$

Let $r = \frac{1}{\lambda}$ then

$$-\frac{\partial\psi}{\partial x} = \frac{(\psi_1-\psi_o)}{a}(1+r) - \frac{(\psi_2-\psi_o)}{a}\frac{1}{(1+r)} \tag{3.9}$$

or

$$\frac{\partial\psi}{\partial x} = \frac{(\psi_o-\psi_1)}{a}(1+r) - \frac{(\psi_o-\psi_2)}{a}\frac{1}{(1+r)} \tag{3.10}$$

3.2 Relaxation Technique

A simple iteration technique which is very convenient, when a digital computer is employed, has been used for this study. The technique mainly consists of the following steps:

(1) Compute residue R_{ij} for all points within flow boundaries in accordance with numerical sequence.

(2) Raise the value of ψ_{ij} there by the amount R_{ij}.

(3) With new value of ψ_{ij}, compute residue $R_{i,j+1}$ of all neighboring points and so on.

(4) Repeat the process till the residues computed are all within an allowable limit.

A simple illustration is shown in Figure 3d.

$$R^o_{2,2} = \psi^o_{2,1} + \psi^o_{2,3} + \psi^o_{1,2} + \psi^o_{3,2} - 4\psi^o_{2,2}$$

$$\psi^1_{2,2} = \psi^o_{2,2} + R^o_{2,2}$$

$$R^o_{2,3} = \psi^1_{2,2} + \psi^o_{2,4} + \psi^o_{1,3} + \psi^o_{2,3} - 4\psi^o_{2,3}$$

$$\psi^1_{2,3} = \psi^o_{2,3} + R^o_{2,3}$$

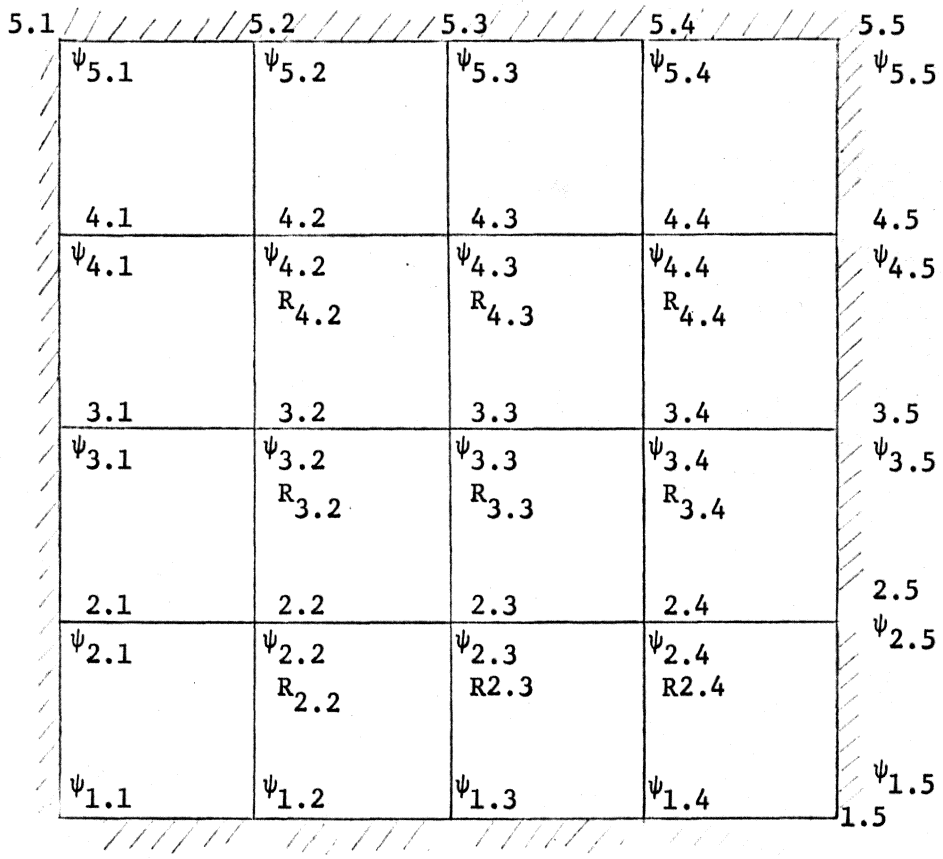

Figure 3d Finite Difference Grid Network

Where the superscript is used to indicate the sequence of the approximation involved in the value at any stage of calculation.

There are some other modified techniques that are often used to speed up the relaxation process, such as over relaxation, under relaxation, group and block relaxation. For instance, it could happen that every time the largest residue is reduced to zero, the other residues are increased. Thus, instead of reducing the largest to zero, we may over relax it to less than zero, so that when the other residues are relaxed, the last residue will come back to zero. This technique is called over-relaxation. By the same token, if by reducing one residue, the other residues are also reduced, then under-relaxation may be used to advantage. Block relaxation changes more than one unknown by the same amount at the same time, whereas group relaxation changes more than one unknown by different amounts at the same time. All of these would help speed up the numerical solution in many occasions when hand calculation is employed. However, if a digital computer is used, the above technique is no longer necessary. Sometimes it might increase computer time and difficulty in programming. The simple relaxation process, presented before, which reduces the residue in accordance with the numbered order of the grid points will be more effective.

CHAPTER IV

CAVITY FLOW AND CAVITY MODEL

4.1 Formation of Cavity

When an obstacle or barrier is placed in a fast moving liquid, the flow usually separates from the obstacle along separating streamlines and the liquid between these separating streamlines constitutes a wake. As the flow velocity increases, the wake becomes gaseous, such a wake is called a cavity. Further increase in velocity or reduction of ambient pressure leads to a large vapor-filled cavity. The formation of gaseous or vapor-filled cavity is of great concern to hydraulic engineers. For instance, a proper selection of spacing and height of artificial roughness elements on the channel bottom will produce effective patterns and shapes of cavities which amplify the form drag and increase flow resistance. Cavity flows possess two important features. First, the cavity surface must always be concave with respect to the center of the cavity. Second, the density ρ of the main fluid must be much larger than the density ρ' of the mixture of vapor and gases in the cavity. The most important parameter governing the form of the cavity and the flow as a whole is the so called cavitation number

$$K = \frac{P_o - P_c}{\frac{1}{2}\rho V_o^2} = \frac{V_c^2}{V_o^2} - 1$$

where P_o is the ambient pressure of the approaching flow, P_c is the cavity pressure, V_0 is the velocity of undisturbed approaching flow and V_c is the velocity along the cavity. For instance, Kirchhoff's flow represents only the limiting case of a cavity flow with $K = 0$. In this flow the cavity extends to infinity. The mathematical and physical properties of steady cavity flows with $K \neq 0$ are not well established. If $K < 0$ the velocity on the free streamline is less than that in the undisturbed flow, and it is presumably necessary for the point of detachment of a free streamline from the body to be in the low-velocity region at the rear of the body. A numerical solution for two-dimensional cavity flow with $K < 0$ was obtained by Southwell and Vaisey as shown in Figure 4a. Cavities for which $K > 0$ are of real physical interest, because a steady cavity which forms in order to avoid the occurrence of a tension zone in the fluid is necessarily one in which the pressure in the cavity is a minimum in the flow field. If K increases the cavity shape becomes more finite as shown in Figure 4b obtained from "Fluid Dynamics" by Batchelor (14).

4.2 Cavity Models

In the analysis of cavity flow problems, four types of models are frequently used. These are the Helmholtz-Kirchhoff model; reentrant jet model, Riabouchinsky's mirror-image model and the notched hodograph model. All of the models are based on the assumption of free streamline theory. For the Helmholtz-

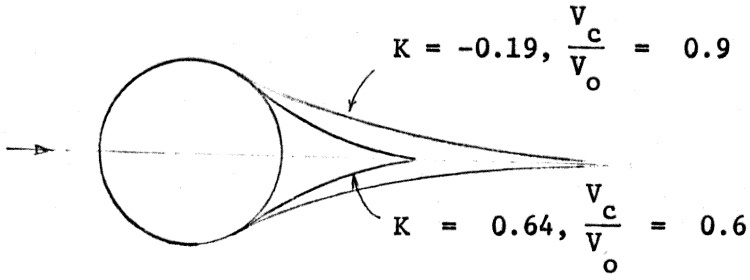

Figure 4a Cusped Wake Model (From Ref. (2))

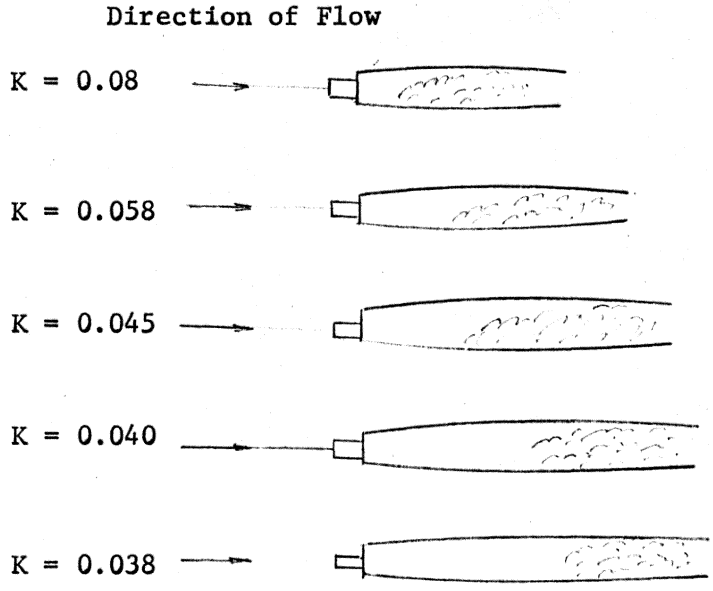

Figure 4b Influence of Cavitation Number on Cavity (From Ref. (14))

Kirchhoff model, the free streamline velocity V is assumed equal to that of approaching undisturbed flow V_∞, i.e., $V_c = K'V_\infty$, where $K' = 1$ for Helmholtz-Kirchhoff model. The deficiency of this model lies in the fact that the cavity pressure P_c is taken to be the same as that in the oncoming flow which leads to a predicted wake of infinite length. The predicted drag force of a normally-placed flat plate is about half that found experimentally. This situation would not occur if the velocity along the free streamline is permitted to exceed that of the approaching flow and a negative base pressure coefficient is allowed. The other three models overcome this difficulty by allowing $K' > 1.0$. The drag and the location of the free streamline in the Helmholtz-Kirchhoff model are found as

$$P = \frac{1}{2} \rho V_o^2 \ell \frac{2\pi}{4+\pi} .$$

$\frac{2\pi}{4+\pi} \approx 0.88$ is called the drag coefficient of the plate. And,

$$\frac{x}{c} = \frac{2}{\pi+4} (\cos\alpha\cot\alpha - \ell n\cot \frac{\alpha}{2})$$

$$\frac{y}{c} = \frac{4}{\pi+4} (\csc \alpha + \frac{\pi}{4})$$

with α varying between $\frac{\pi}{2}$ and 0 as x and y increase (see Figure 4c).

One of the most successful cavity models is the Efros reentrant jet model as shown in Figure 4d. This model allows the free streamline to turn inwards and to produce a jet moving toward the plate. This model is intended to give a correct representation of the flow in front of the flat plate, and is based on the assumption that the

flow picture at the end of the cavity has a small influence on the velocity field in the vicinity of the body. The dimensions of the cavity region for the model are determined as follows: the cavity length a is the distance from the plate to that point of the cavity surface with a vertical surface, and the cavity width b is the distance between the points of the cavity surface with horizontal tangents.

The Riabouchinsky "mirror-image" model is shown in Figure 4c. This model, as does the reentrant jet model, allows calculation of not only the drag forces acting on the body, but also the order of magnitude of the cavity dimension. Riabouchinsky assumed that the whole flow field is symmetrical about transverse plane, and that in effect an image plate exists at a certain distance downstream from the first plate. The second plate takes care of the cumulative effects of friction and eddy motion in the wake behind the body. The pressure in the region between the plates is below that in the approaching stream. Since the free streamline velocity is greater than V_∞, the maximum length of the wake is now finite. This model like the reentrant jet model also has improved the prediction of drag force and base pressure. A suitable choice of the plate spacing led to a satisfactory result, and the flow picture ahead of the mid-plane appeared reasonable.

The length of the cavity is obtained as

$$a = \frac{2\phi_o}{V_o}\left[\frac{1}{K^2}E - \frac{1-k^2}{k^2}K\right]$$

and the width of the cavity is

$$b = \ell + \frac{2\phi_o}{V_o} \frac{(1-k^2)^{\frac{1}{2}}}{1+(1-k^2)^{\frac{1}{2}}}$$

where K and E are the complete elliptic integrals of the first and second kind with modulus k_1 as shown in the text of Gurevich (15).

The other improved hodograph flow model is the notched model presented in Figure 4f. In this model the free streamline velocity V along CD and PQ is larger than the approaching velocity V_∞, and after D and Q the velocity is decreased slowly to the magnitude V_∞. The decrease of V to V_∞ is due to dissipation of energy.

For all these models no gravitational effect is considered. The cavity model used in this study is primarily based on Helmholtz-Kirchhoff's model ($P_c = P_\infty$) with gravitational effects included. It is expected that with gravitational effects, the cavity surface will be pulled down to form a finite cavity shape as shown in Figure 4g. The cavity model is then modified with $P_c > P_\infty$ and $P_c < P_\infty$, and also $P_c = d_c$ as shown in Reference (11).

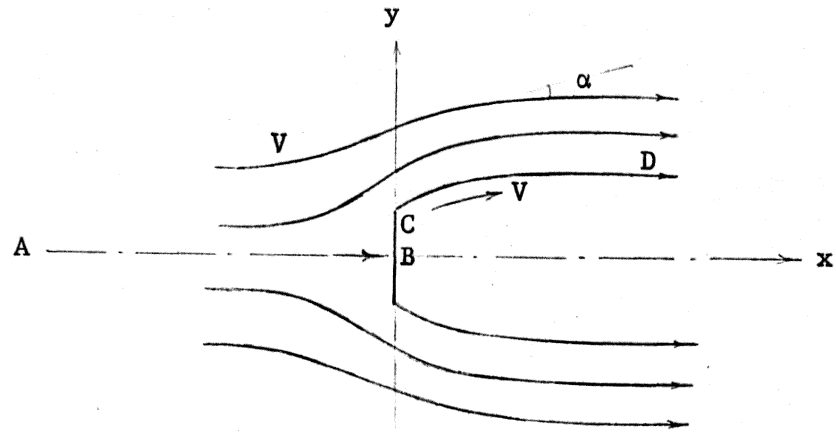

Figure 4c Helmholtz-Kirchhoff Model

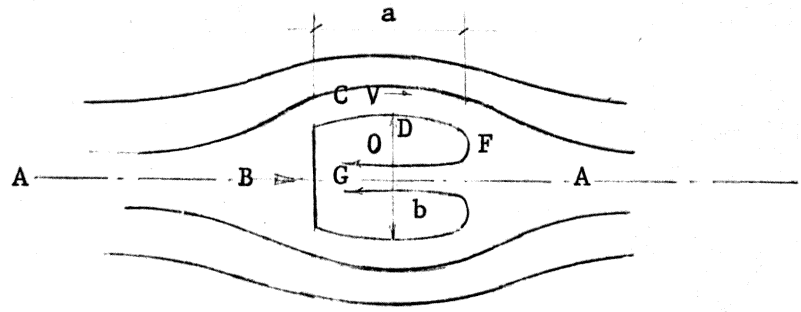

Figure 4d Reentrant Jet Model

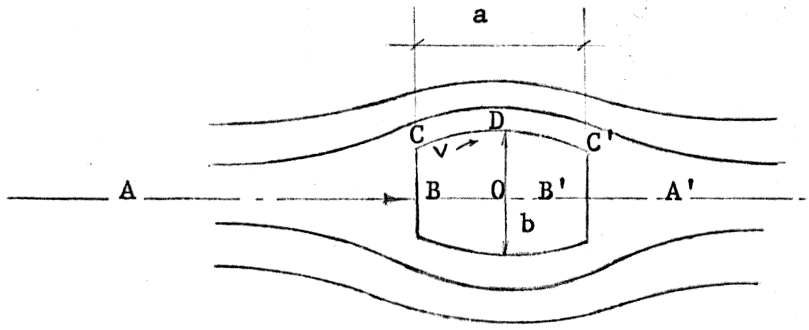

Figure 4e Riabouchinsky Image Model

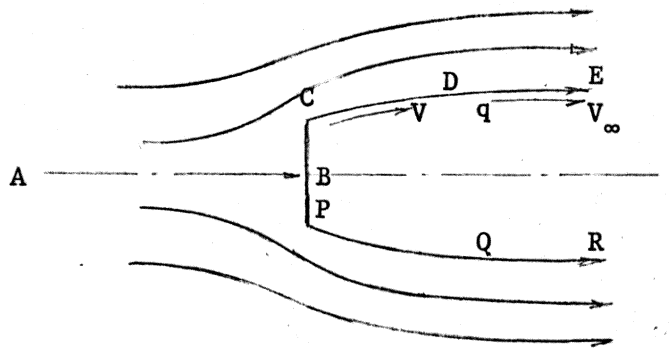

Figure 4f Notch Hodograph Model

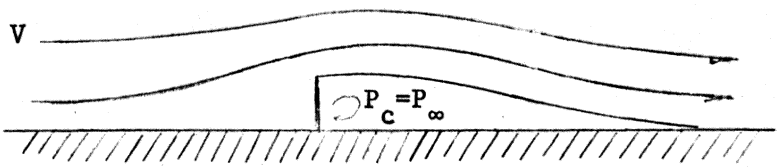

Figure 4g Helmholtz-Kirchhoff Model with Gravity Effect (Predicted shape)

CHAPTER V

MATHEMATICAL MODEL FORMULATION

5.1 Statement of the Problems

As mentioned before, the primary aim of this study is to use the realxation method to solve the cavity flow problem including gravitational effects. With the assumptions made before, this study reduces to finding the solution of the Laplace equation with the specified boundary conditions. Referring to Figure 5a, we see that the Laplace equation

$$\nabla^2\psi = \frac{\partial^2\psi}{\partial^2 x^2} + \frac{\partial^2\psi}{\partial y^2} = 0 \tag{5.1}$$

must be satisfied everywhere within the boundary. While

$$\left.\begin{aligned} \psi &= \text{const.} \\ \left(\frac{\partial\psi}{\partial n}\right)^2 &= \left(\frac{\partial\psi}{\partial x}\right)^2 + \left(\frac{\partial\psi}{\partial y}\right)^2 = 2gy \end{aligned}\right\} \tag{5.2}$$

and

$$\left.\begin{aligned} \psi &= \text{const.} \\ \left(\frac{\partial\psi}{\partial n}\right)_c^2 &= \left(\frac{\partial\psi}{\partial n}\right)_o^2 - 2gd_c \end{aligned}\right\} \tag{5.3}$$

must be satisfied along the free surface and the cavity surface, respectively. Y is the vertical distance between the energy line and the free surface and d_c is the vertical distance between the cavity surface and the channel bottom as shown in Figure 5a.

5.2 Dimensionless Expression of Governing Equations

The reduction of Laplace's equation into a dimensionless form is very convenient. Since numerical values of the dimensionless stream function ψ can be selected at will in terms of the flow characteristic either upstream or downstream from the obstacle, a lot of work in preparing the computer input can be saved. Let us assume:

$$X = X'D,\ y = y'D,\ n = n'D,\ h = h'D,\ dc = dc'D,\ \psi = \psi' F_o\sqrt{2gD^3}$$

where D is some representative dimension of the fixed boundary. Then

$$\frac{\partial\psi}{\partial x} = \frac{\partial\psi}{\partial\psi'}\frac{\partial\psi'}{\partial x'}\frac{\partial x'}{\partial x} = (F_o\sqrt{2gD^3})\frac{1}{D}\frac{\partial\psi'}{\partial x'} = F_o\sqrt{2gD}\ \frac{\partial\psi'}{\partial x'}$$

$$\frac{\partial^2\psi}{\partial x^2} = \frac{\partial}{\partial x}\{(F_o\sqrt{2gD})\frac{\partial\psi'}{\partial x'}\} = F_o\sqrt{2gD}\ \frac{\partial^2\psi'}{\partial x'^2}\frac{\partial x'}{\partial x} = F_o\sqrt{\frac{2g}{G}}\ \frac{\partial^2\psi'}{\partial x'^2}$$

similarly,

$$\frac{\partial\psi}{\partial y} = F_o\sqrt{2gD}\ \frac{\partial\psi'}{\partial y'},\quad \frac{\partial^2\psi}{\partial y^2} = F_o\ \sqrt{\frac{2g}{D}}\ \frac{\partial^2\psi'}{\partial y'^2}$$

$$\frac{\partial\psi}{\partial n} = (F_o\sqrt{2gD})\frac{\partial\psi'}{\partial n'}$$

or

$$V = V'\ (F_0\sqrt{2gD})$$

The Laplace equation in dimensionless form becomes

$$\nabla^2\psi = F_o\sqrt{\frac{2g}{D}}\left(\frac{\partial^2\psi'}{\partial x'^2}+\frac{\partial^2\psi'}{\partial y'^2}\right) = 0$$

or

$$\nabla^2\psi' = \frac{\partial^2\psi'}{\partial x'^2}+\frac{\partial^2\psi'}{\partial y'^2} = 0$$

Along the free surface, the boundary conditions in dimensionless form are

$$\psi = \psi' F_o\sqrt{2gD^3} = K = \text{const.}$$

or

$$\psi' = k'$$

where

$$k' = \text{const.} = \frac{K}{F_o\sqrt{2gD^3}}$$

and

$$\left(\frac{\partial\psi}{\partial n}\right)^2 = \left(F_o\sqrt{2gD}\right)^2\left(\frac{\partial\psi'}{\partial n'}\right)^2 = 2gy'D$$

therefore

$$\left(\frac{\partial\psi'}{\partial n'}\right)^2 = \frac{y'}{F_o^2}$$

Equation (5.2) thus becomes

$$\left.\begin{aligned}\psi' &= \text{const.}\\ \left(\frac{\partial\psi'}{\partial n'}\right)^2 &= \frac{y'}{F_o^2}\end{aligned}\right\} \qquad (5.4)$$

Along the cavity surface, the dimensionless boundary conditions become:

$$\left(\frac{\partial\psi'}{\partial n'}\right)_c^2 \left(F_o\sqrt{2gD}\right)^2 = \left(\frac{\partial\psi'}{\partial n'}\right)_o^2 \left(F_o\sqrt{2gD}\right)^2 - 2g\, d_c' D$$

therefore

$$\left(\frac{\partial\psi'}{\partial n'}\right)_c^2 = \left(\frac{\partial\psi}{\partial n'}\right)_o^2 - \frac{d_c'}{F_o^2}$$

Equation (5.3) thus becomes

$$\left.\begin{aligned} \psi' &= \text{const.} \\ \left(\frac{\partial\psi'}{\partial n'}\right)_c^2 &= \left(\frac{\partial\psi'}{\partial n'}\right)_o^2 - \frac{d_c'}{F_o^2} \end{aligned}\right\} \qquad (5.5)$$

If we choose $D = h_0/2$, where h_0 is the water depth at an upstream uniform section, then $h_0' = h_0/D = 2$ and

$$V = V' F_0\sqrt{2gD} = V' F_0\sqrt{gh_0}$$

or

$$V' = \frac{V}{F_o\sqrt{gh_0}} = \frac{V}{V_o}$$

where

$$F_o = \frac{V_o}{\sqrt{gh_o}} \quad \text{(Froude Number)}$$

At upstream sections where uniform flow conditions exist

$$V = V_0$$

therefore

$$V' = \frac{V_0}{V_0} = 1$$

The Ψ' values at free surface will be

$$\psi' = V'_o h'_o = 1 \times 2 = 2$$

5.3 Method of Solution

A computer program was written to solve the dimensionless form of Laplace's equation with different boundary conditions specified. The method of solution developed in this program consists of the following steps:

(1) Define all flow boundaries including fixed and free boundaries: In the analysis of free streamline flow problems the location of the free streamline must first be assumed. If the assumed location is far from the true one the solution might not converge. Therefore, reasonable locations and surface profiles must be assumed. To determine upstream and downstream boundaries, one must locate both boundaries far away from the point of the disturbance where uniform flow conditions exist. Referring to Figure 5b, we selected the ratios $\frac{L_1}{EH} = 20$ and $\frac{L_2}{EH} = 20$ for the first trial. The ratios are then gradually increased till a further increase in the ratios would not effect the surface profiles and the cavity length. The sections

are then fixed for the final solution. The same principle is applied for the determination of mesh sizes. The grid spacing is based on the assumption that a linear variation of properties exists between two neighboring points. Therefore, whenever the assumption of linearity is violated the mesh size would be reduced.

(2) Assign initial values of ψ within the flow field: $\psi = 0$ along channel bottom and $\psi = 2$ along free surface are specified. The ψ values within the flow field are then obtained by linear interpolation between the value on the free surface and that on the channel bottom.

(3) Successive reduction of residues by relaxation process: Following the assignment of initial ψ values, the residues at every point except at the boundary are computed throughout the whole region. The residues are then reduced successively from the lower left corner to the upper right corner, and the process is repeated till the required accuracy is obtained. The allowable error for residue R_0 is limited to less than $0.005\ \psi_o$.

(4) When the relaxation process is completed, the velocities along the free surface as well as the cavity surface are computed.

Since

$$\frac{\partial \psi}{\partial n} = \frac{\partial \psi}{\partial x} \cos \theta + \frac{\partial \psi}{\partial y} \sin \theta \qquad (5.6)$$

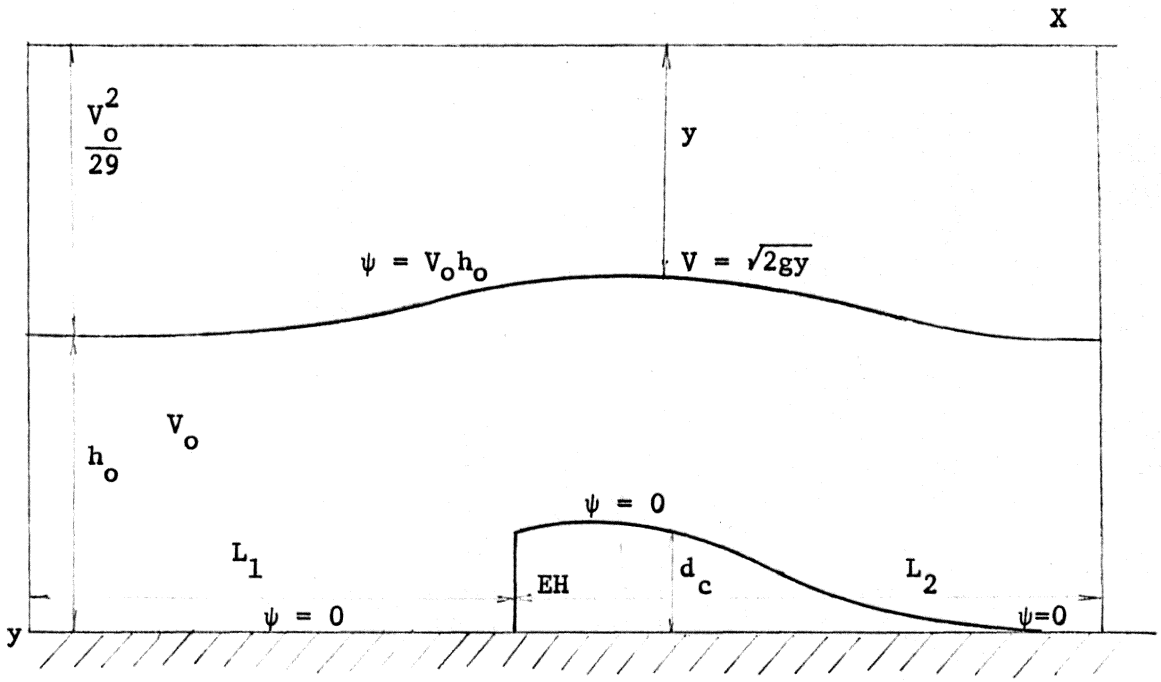

Figure 5a Physical Plane

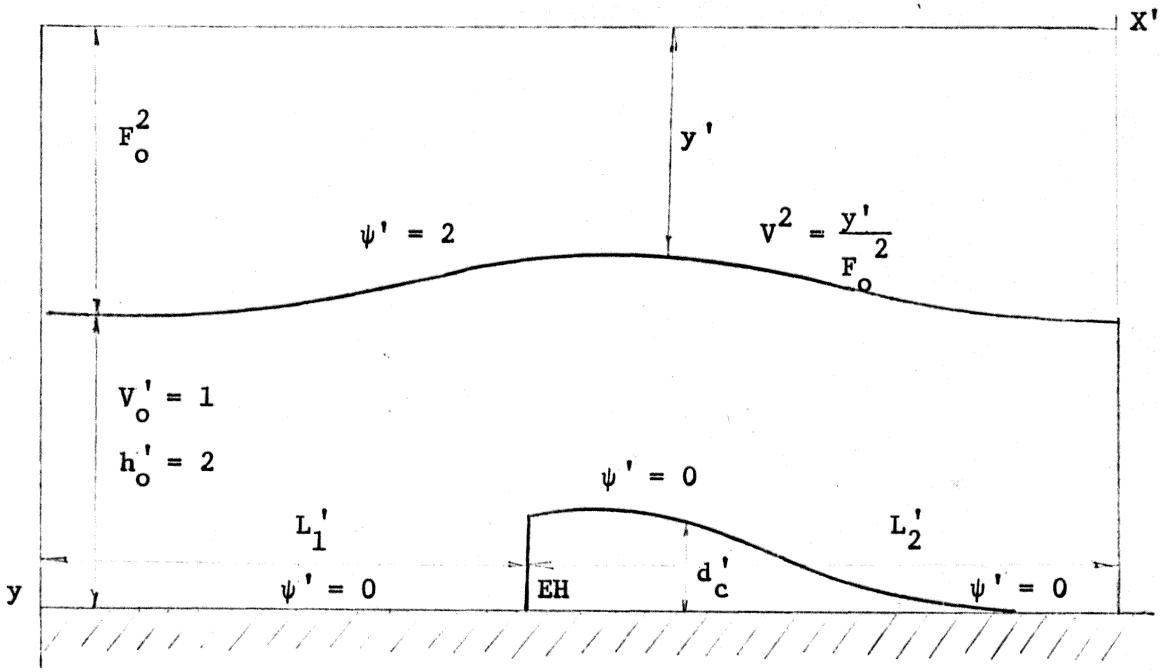

Figure 5b Normalized Plane

$$\frac{\partial \psi}{\partial s} = \frac{\partial \psi}{\partial y} \cos \theta - \frac{\partial \psi}{\partial x} \sin \theta \qquad (5.7)$$

(see Figure 5c). Thus, when $\frac{\partial \psi}{\partial s} = 0$, from equation (5.7), we obtain

$$\frac{\partial \psi}{\partial y} \cos \theta = \frac{\partial \psi}{\partial x} \sin \theta \ , \qquad \frac{\partial \psi}{\partial x} = \frac{\partial \psi}{\partial y} \cot \theta$$

Substitute in equation (5.6)

$$\frac{\partial \psi}{\partial n} = \frac{\partial \psi}{\partial y} \cot \theta \cos \theta + \frac{\partial \psi}{\partial y} \sin \theta$$

multiply both sides by sin θ

$$\sin \theta \ \frac{\partial \psi}{\partial n} = \frac{\partial \psi}{\partial y} \cos^2 \theta + \frac{\partial \psi}{\partial y} \sin^2 \theta = \frac{\partial \psi}{\partial y} (\cos^2 \theta + \sin^2 \theta)$$

therefore

$$\frac{\partial \psi}{\partial n} = \frac{1}{\sin \theta} \frac{\partial \psi}{\partial y} \qquad (5.8)$$

similarly

$$\frac{\partial \psi}{\partial n} = \frac{1}{\cos \theta} \frac{\partial \psi}{\partial x} \qquad (5.9)$$

The last two equations are used to find velocity along the free surface and the cavity surface. The computed velocities are then used to check with boundary conditions specified, i.e., equations: (5.4) and (5.5).

(5) Adjust location of free boundaries if boundary conditions for both surfaces are not satisfied. Let

$$\Delta E_f = \{(\frac{\partial \psi'}{\partial n'})^2 - \frac{y'^2}{F_o}\} \quad \frac{1}{(\frac{y'^2}{F_o})}$$

and

$$\Delta E_c = \{(\frac{\partial \psi'}{\partial n'})_c^2 - (\frac{\partial \psi'}{\partial n'})_o^2 + \frac{d_c'}{F_o^2}\} \frac{1}{\{(\frac{\partial \psi'}{\partial n'})^2 - \frac{d_c'}{F_o^2}\}}$$

where ΔE_f is the percent error for free surface and ΔE_c is the percent error for cavity surface.

If $|\Delta E_f|$ or $|\Delta E_c|$ is greater than 0.01 the locations of free streamlines have to be adjusted. The amount of adjustment is based on the sign and magnitude of ΔE. For instance, if ΔE_f is positive, the elevation of free surface must be decreased; if negative, it must be increased. As to cavity surface, the opposite is true. If ΔE_c is positive the elevation must be increased, while if negative it must be decreased.

To adjust the position of free surface, the following steps are employed: First, equation (5.9) is used to compute the velocity along free surface, and then the percent error ΔE_f is computed. If the error is greater than the allowable, the position of the surface must be corrected, the correction will be

$$Y_{i,j}^1 = Y_{i,j}^o + C\Delta E_{i,j}$$

where C is a constant used to limit the amount of adjustment, $Y_{i,j}^1$ is the revised location and $Y_{i,j}^o$ is the present location.

If $Y^1_{i,j} < Y_{i,1}$ and $Y^1_{i,j+1} > Y_{i,1}$ (see Figure 5d) the free surface must intersect with the horizontal string between column (i,j) and column (i,j+1). Therefore, the position of the intersection point must be computed, the position of the point will be

$$X_{i,N} = X_{i,j+1} - \Delta x \frac{Y^1_{i,j+1} - Y_{i,1}}{Y^1_{i,i+1} - Y^1_{i,j}}$$

$$Y_{i,N} = Y_{i,1} \text{ , and } \psi_{i,N} = 2.0$$

obtained by linear interpolation. If $Y_{i,1} < Y^1_{i,j} < Y_{i+1,1}$ then

$$Y_{i+1,j} = Y^1_{i,j} \text{ and } \psi_{i+1,j} = 2.0$$

similarly, if $Y_{i-1,} < Y^1_{i,j} \leq Y_{i,1}$, then

$$Y_{i,j} = Y^1_{i,j} \text{ and } \psi_{i,j} = 2.0$$

the same principle is applied for the cavity surfaces but the difference is that if $Y_{i,1} \leq Y^1_{i,j} < Y_{i+1,1}$

$$Y_{i,j} = Y^1_{i,j}, \text{ and } \psi_{i,j} = 0$$

and if $Y_{i-1,1} \leq Y^1_{i,j} < Y_{i,1}$, then

$$Y_{i-1,j} = Y^1_{i,j}, \text{ and } \psi_{i-1} = 0 .$$

The boundary conditions for the separation point are the same as that of the cavity surface, (see Equation (5.3)). The value of the

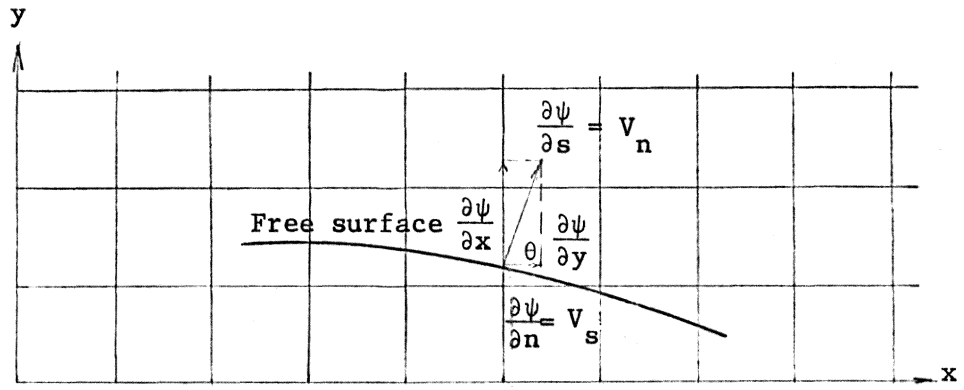

Figure 5c Velocity Vectors Used in Adjustment of Free Surface

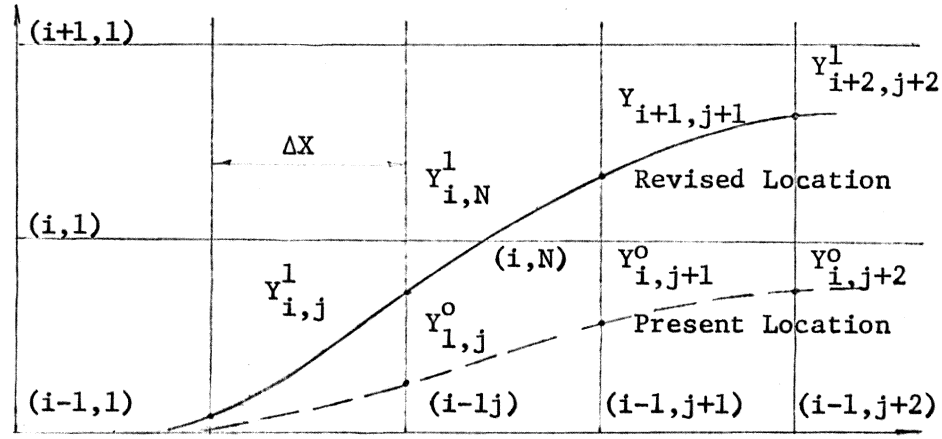

Figure 5d Adjustment of Free Surface

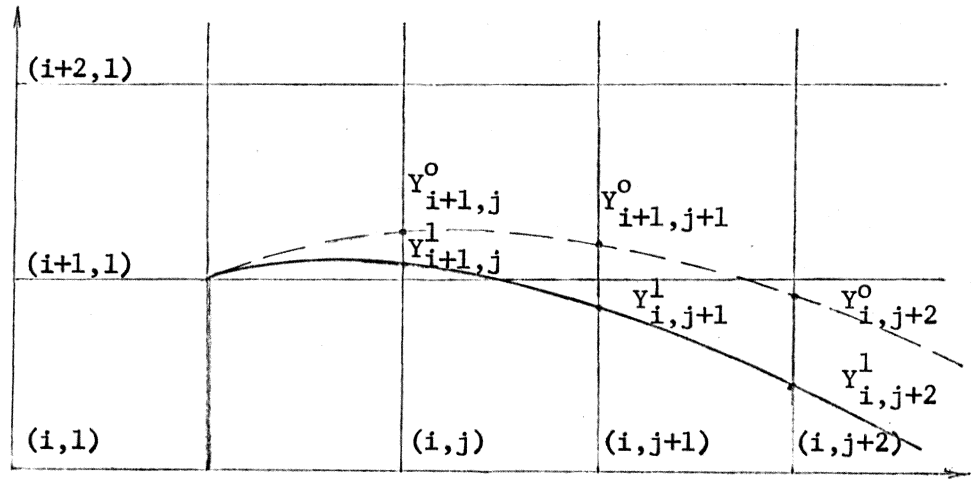

Figure 5e Adjustment of Cavity Surface

stream function ψ at the separation point remains constant and always equals zero ($\psi = 0$). Since the separation point is a fixed boundary point, no residue is computed or distributed to that point.

The difficulty in developing a systematic method of adjustment arises from the fact that mutual interference exists between the adjustments of free surface and cavity surface. Thus it is necessary to find the correlation of their interference. The following different approaches were attempted to find a desirable method of adjustment.

(i) Assume cavity surface as a fixed boundary. Adjustments are made repeatedly for free surface only. When the boundary conditions for free surface are satisfied, the free surface is then fixed, and begin adjusting the cavity surface. Reverse the process till boundary conditions for both surfaces are satisfied.

(ii) The second approach is a modification of the first one. Fix cavity surface first, and adjust free surface only. If the adjustment of free surface will reduce both errors ΔE_f and ΔE_c, then continuous adjustments are made for free surface only. If the adjustment of free surface will result in increasing error in cavity surface, the free surface will be fixed and begin adjusting the cavity surface. While if the adjustment of cavity surface results in the increase of error in free surface the cavity surface will be fixed again. Repeat the process till the errors for both surfaces are satisfied.

(iii) Adjust both surfaces at the same time with the same amount of adjustment. The errors for both surfaces are computed and summed up. The amount of adjustment is made equally for both surfaces in accordance with the error summed up.

(iv) Adjust both surfaces at the same time with different amounts of adjustment. The amount of adjustment for each surface is made in accordance to its own error computed.

CHAPTER VI

RESULTS

6.1 Computer Results

Sixteen primary cases with cavity pressure $P_c = P_0$ were investigated. The element heights used were EH = 0.4, 1.8, 1.2 and 1.6. For each element height, four flow conditions (Froude Number N_F = 2, 4, 6 and 8) were applied. The cavity and free surface profiles are shown in Figure 6a to 6d, and several additional cases, $P_c \leq P_0$ and $P_c > P_0$, are also included. From the plots, the following results are observed.

(1) Cavity surfaces for all 16 primary cases are all convex with respect to the center of cavity, and no finite length of cavity can be obtained.

(2) The effect of Froude Number N_F, the major concern in this study, cannot be distinguished.

(3) At the point of separation where a weak singularity exists, the error is large and cannot be eliminated. The error ΔE_c computed at the point of separation is equal to 1.35 on the average. Similar difficulties have also been reported by others, (See References 8 and 9). Street pointed out that the free streamline error always had a large value near the separation point.

(4) The cavity length would become finite if $P_c > P_\infty$. However, the cavity shape would be even more cusped and the correct free surface profile may not be obtained.

(5) If the cavity pressure $P_c = 0.0$ or $P_c < 0.0$, the cavity

shape would become concave with respect to its center. Nevertheless, no apparent inflexion point can be found to determine the cavity length.

(6) Maximum water surface elevation occurs at downstream side of elements with distances equal to three to five times element height, and the effect of Froude Number on free surface elevation again cannot be distinguished, (see Figure 6f).

(7) The last approach of method of adjustment mentioned in Chapter V has a faster speed of convergence in relaxation solution and was used here.

(8) The mesh size a = 0.4 was found small enough for present study; a finer mesh was not found necessary.

(9) The upstream boundary located at the distance L_F from the element with ratio $\frac{L_1}{EH}$ = 20 is found far enough for all the cases. Further increase in $\frac{L_1}{EH}$ ratio is not necessary. For the downstream boundary the ratio $\frac{L_2}{EH}$ increases where the N_F increases. But $\frac{L_2}{EH}$ = 30 is good enough for all the cases.

(10) The boundary errors DE(j) computed for the jth boundary point is not necessarily the true amount of error to be corrected. It merely is a qualitative indication and adjustment of 1/10 of its amount each time is suitable.

(11) The computer processor time required for each run was about three minutes. The average core storage needed was about 20,000 words. The number of iterations for convergence was limited to 30.

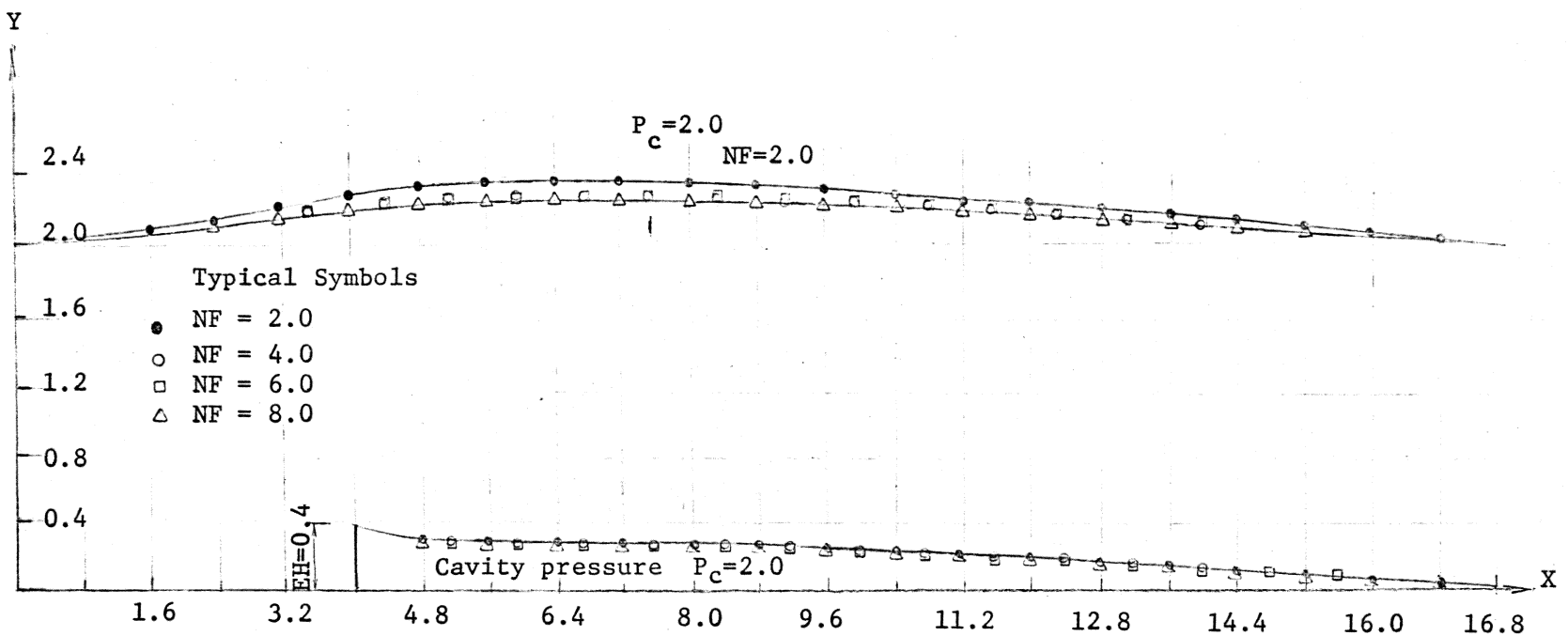

Figure 6a Dimensionless Flow Profiles: (EH = 0.4)

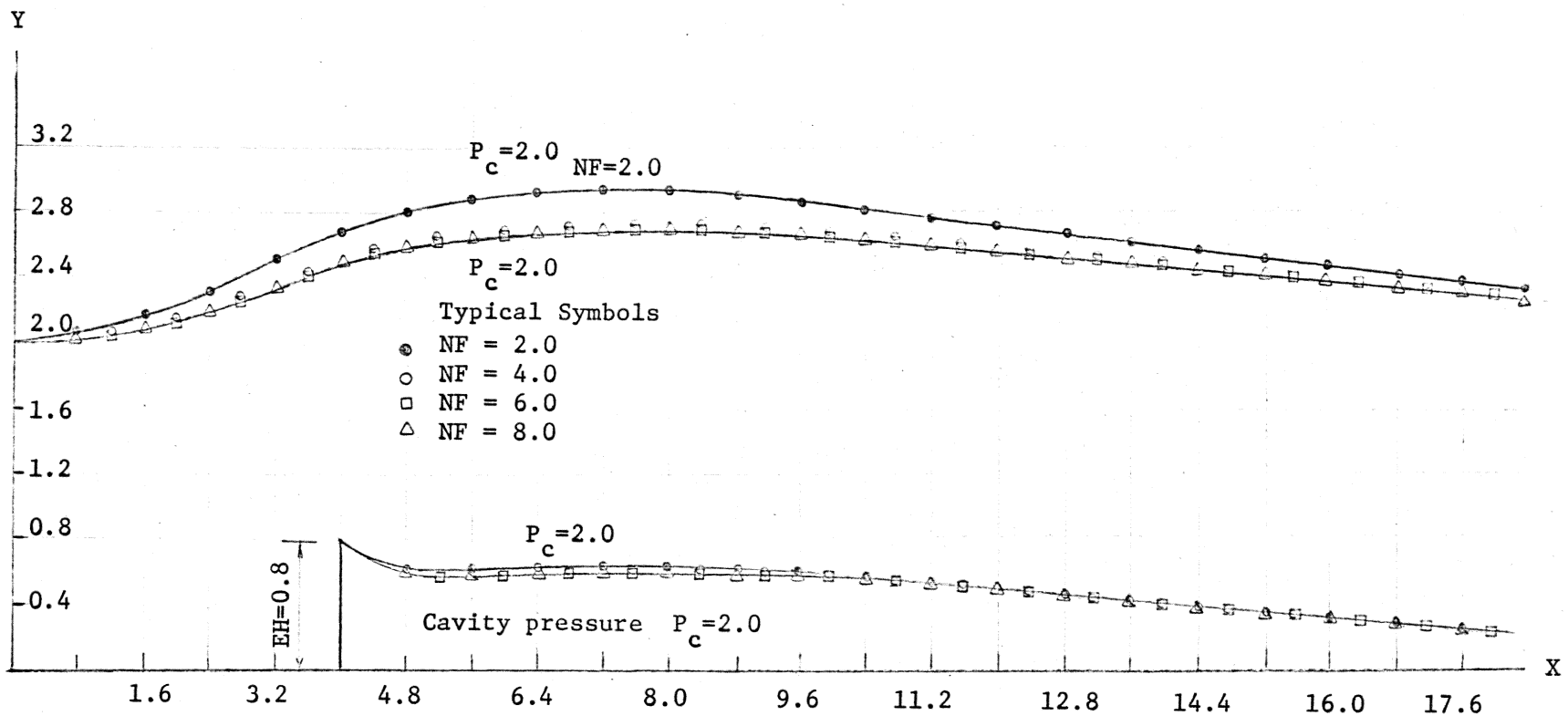

Figure 6b Dimensionless Flow Profiles (EH = 0.8)

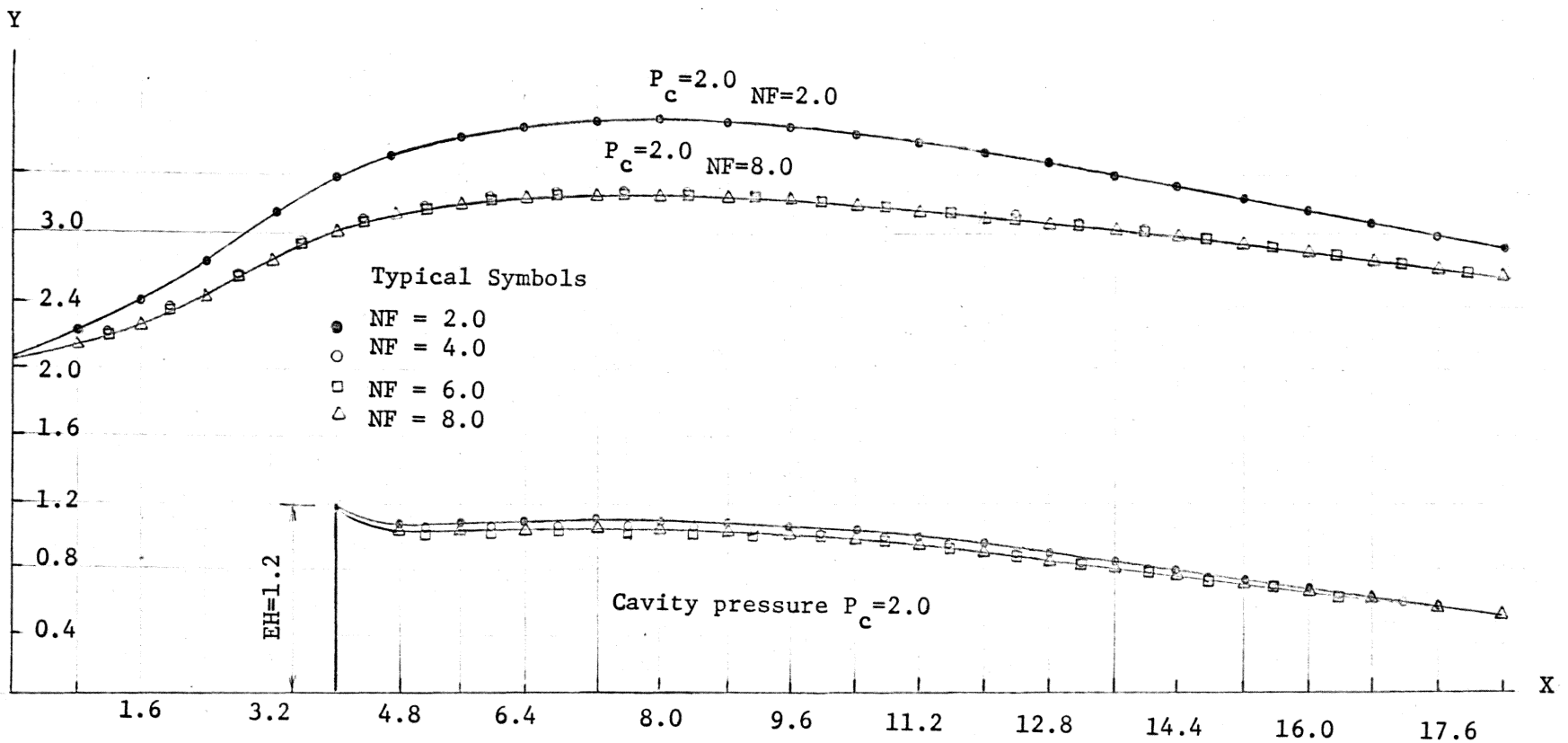

Figure 6c Dimensionless Flow Profiles (EH = 1.2)

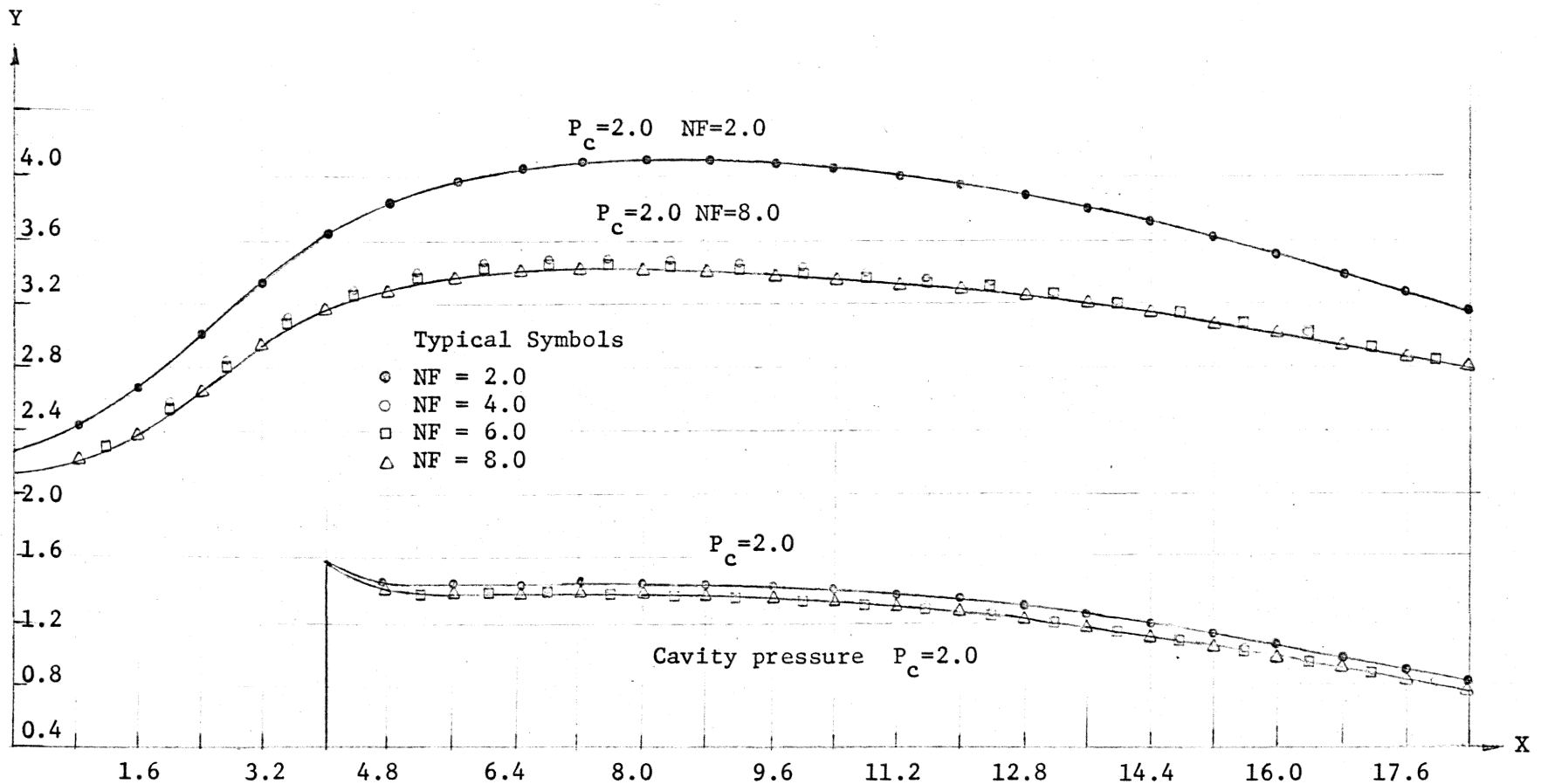

Figure 6d Dimensionless Flow Profiles (EH = 1.6)

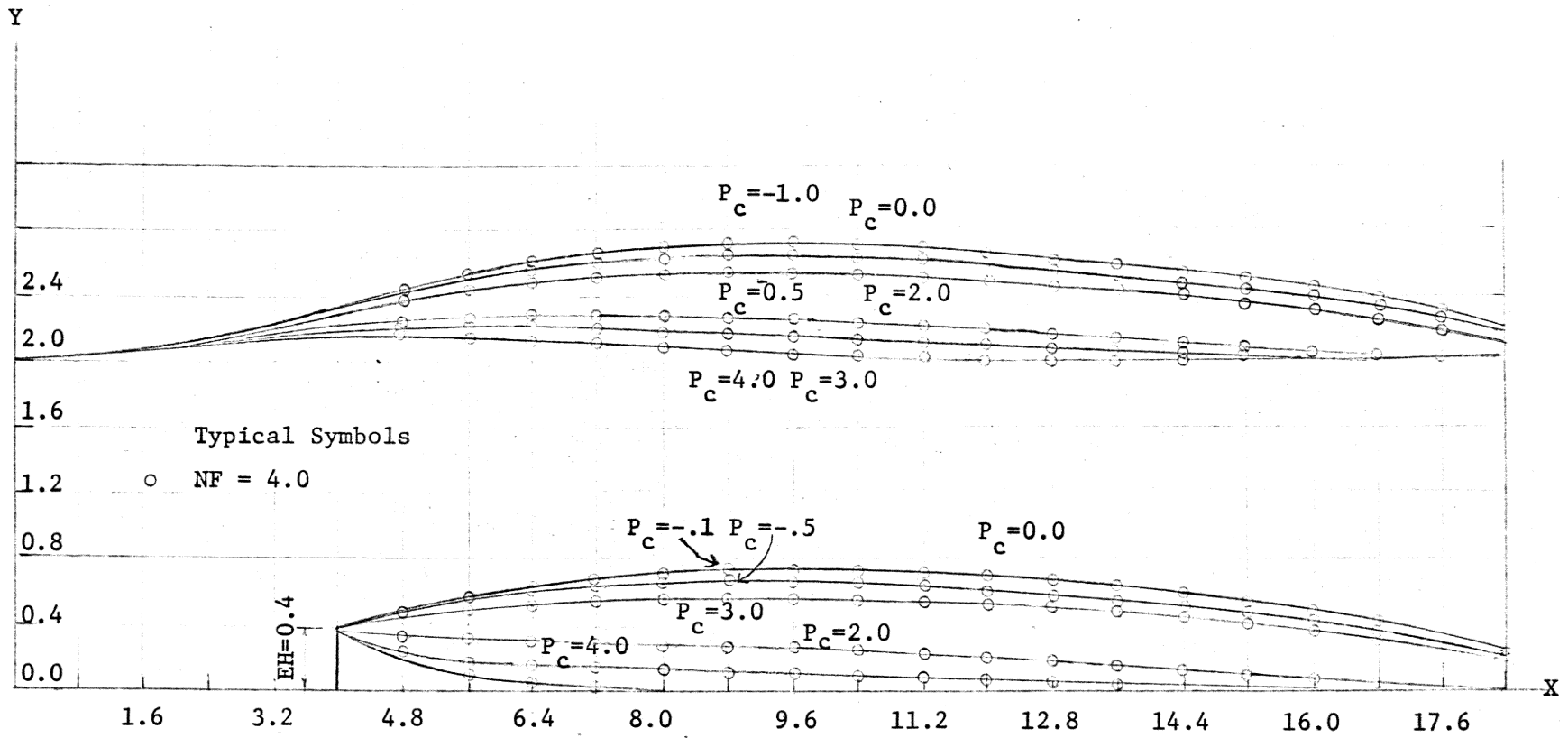

Figure 6e Dimensionless Flow Profiles (EH = 0.4)

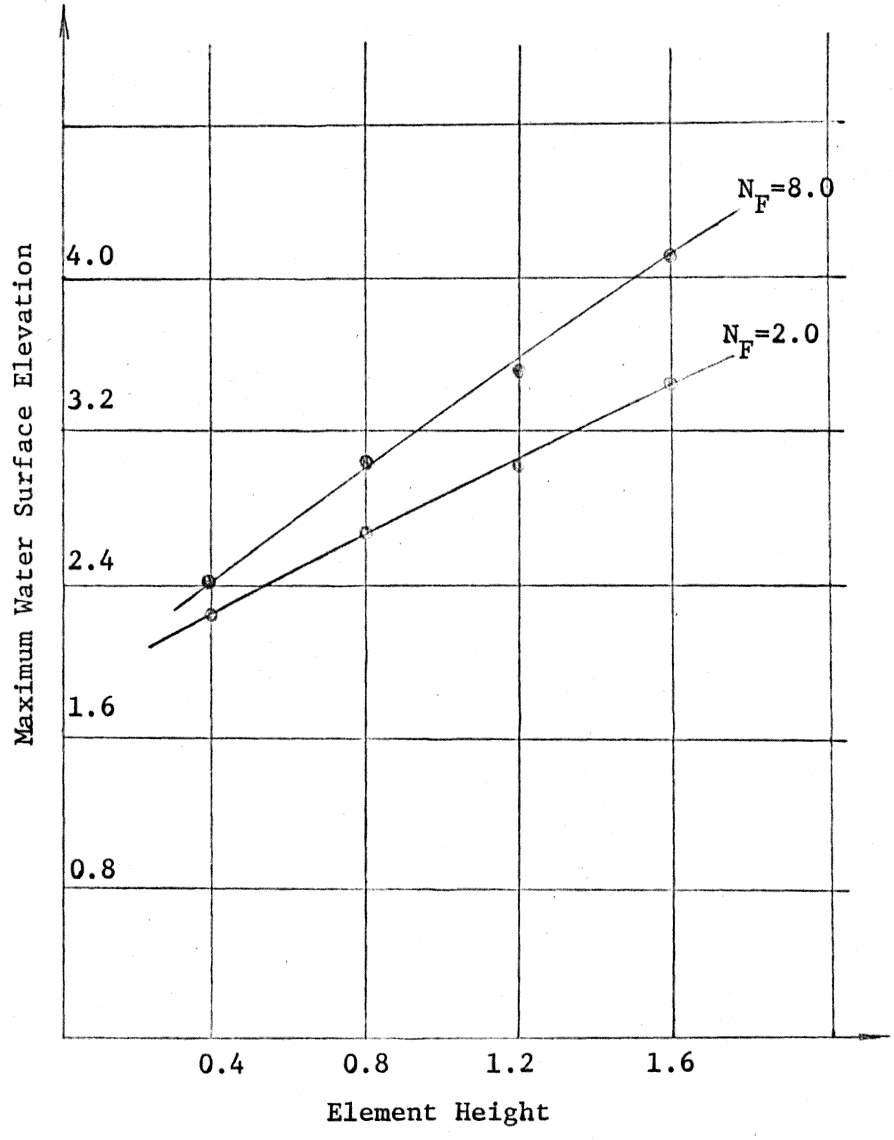

Figure 6f Max. Water Depth vs. Element Height

CHAPTER VII

CONCLUSIONS AND RECOMMENDATIONS

7.1 Conclusions

The cavity model presented in this study was found unsuccessful, because neither the real shape nor a finite length of cavity could be obtained. The reason is that the effect of gravity is far less than the effect of cavity pressure assumed. The effect of gravity would become more dominant if the channel bottom were sloped. This study proves the fact that if $P_c < P_\infty$, regardless of whether it is a free stream line or a free surface problem, no finite length of cavity can be obtained. And if the downstream boundary is not fixed, the more the cavity pressure is reduced the wider will be the opening of the cavity.

This study also confirms the fact that the only way to obtain a finite length of cavity is by use of a cusped wake model, as Southwell did, which requires $P_c > P_\infty$. Nevertheless, the cusped wake model is physically impossible, since the cavity pressure should be the minimum pressure within a given flow field. Besides, the true free surface profile can never be obtained because of the unrealistic cavity shape.

The reason why the Helmholtz Kirchhoff model was used instead of the other two types of models, the Riabouchinsky and the reentrant jet models, is that the former has the simplest boundary conditions, which can be solved easily by the relaxation method. If a reentrant jet model is used, a portion q_1 of the discharge Q would flow back-

ward towards the element, and the value of ψ along the channel bottom downstream of the element would become $\psi = V_c h_1 = q_1$. This is an unknown and would have to be assumed at first. If after relaxation, the computed reentrant jet depth is equal to h_1, then the assumed value of q_1 is correct. If not, it has to be changed. Also, the same problem would be encountered here as in the previous model, i.e., the singularity at the separation point. The adjustment of the surface of the reentrant jet would also complicate the program. Numerical solutions can also be obtained if the Riabouchinsky model is used, but the iteration process might be more complicated than that of the Helmholtz-Kirchhoff model. Referring to Figure 7b, if the Riabouchinsky model is used, the cavity length has to be assumed first. Then relaxation proceeds and the surface is adjusted repeatedly until the boundary errors for both the free surface as well as cavity surface are all within an allowable limit. If the error cannot be reduced in a fixed number of iterations, the cavity length must be changed and the process restarted. Even when the errors are allowable, the cavity length still needs to be changed repeatedly until a further change in the length would not result in any reduction of boundary errors. The correct cavity length should be the one which has the minimum boundary errors. Since for every change in cavity length the same solution process needed by Helmholtz-Kirchhoff model must be used, the computer time would become extravagant. This is the reason why the Riabouchinsky model was not used.

7.2 Recommendations

To find the solution of cavity flows with free surfaces, the relaxation technique can be applied. The success of the method depends on the kind of model used. This study confirms that the Helmholtz-Kirchhoff model is not applicable. Therefore, the other two models (reentrant jet model and Riabouchinsky model) must be considered. If any attempt to obtain a numerical solution is made using the reentrant jet model, it is advised that the transformed plane ($\phi \sim \psi$) be used, since at least, the adjustment of cavity surface would be much easier in the transformed plane than in the physical plane.

The model to be recommended here is the Riabouchinsky model, because it has a reasonable cavity shape and also has simple boundary conditions which can be handled easily with the relaxation method. If the whole model (see Figure 7b) is used, one would encounter a large iteration process and need considerable computer time for the numerical solution. However, if it is assumed that the maximum free surface elevation occurs at the same position (along x-axis) as the cavity surface does (see Figure 7c), we can use a half model to reduce the numerical computation and save computer time. The maximum water depth, as well as the cavity length, obtained by this half model could be good enough for design purposes. The solution can be obtained either in a physical plane or in a transformed plane. The advantage of using the physical plane is that because of its direct approach to the solution, the complex nature of mapping technique can be avoided, and if any errors occur during the computer process,

they are easier to detect in the physical plane than in any other transformed plane. The disadvantage, however, is that because of the existence of irregular strings around the free boundaries, a simple effective adjustment of the boundary locations is difficult. Besides, whenever an extension of the flow region is found necessary, it is more difficult to extend the flow region with irregular strings than with regular strings. The opposite is true for the transformed planes. But it might be more interesting to attempt a numerical solution in transformed planes because it is a more elegant mathematical technique.

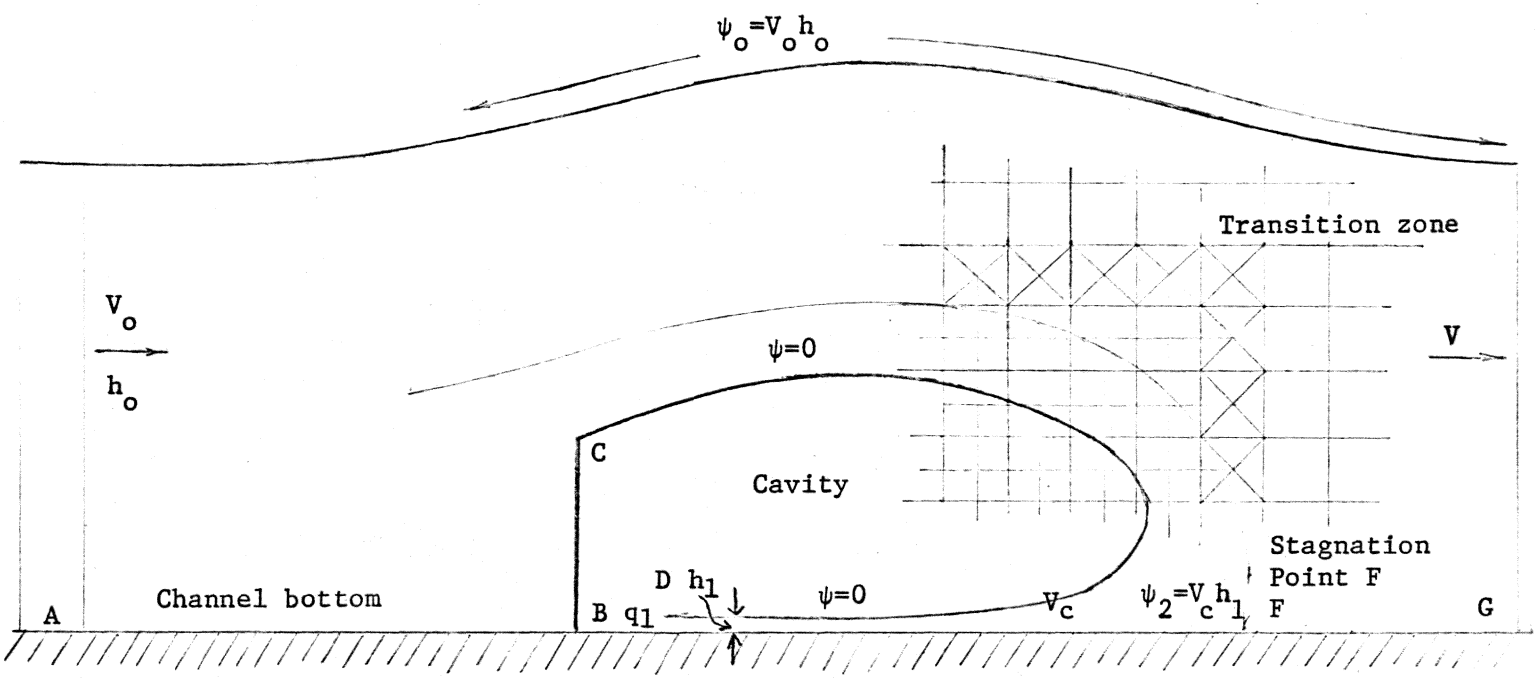

Figure 7a Reentrant Jet Model

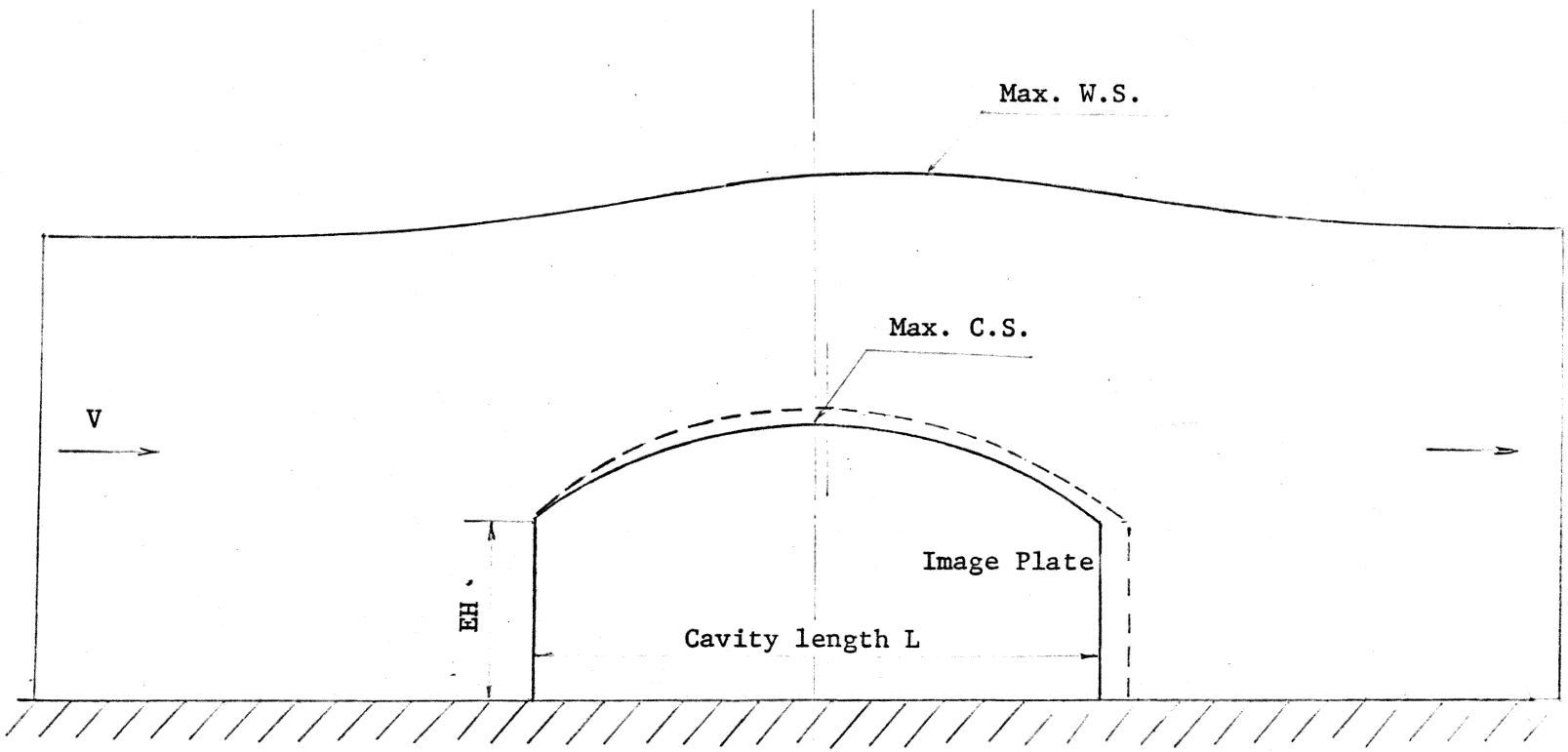

Figure 7b Riabouchinsky Model

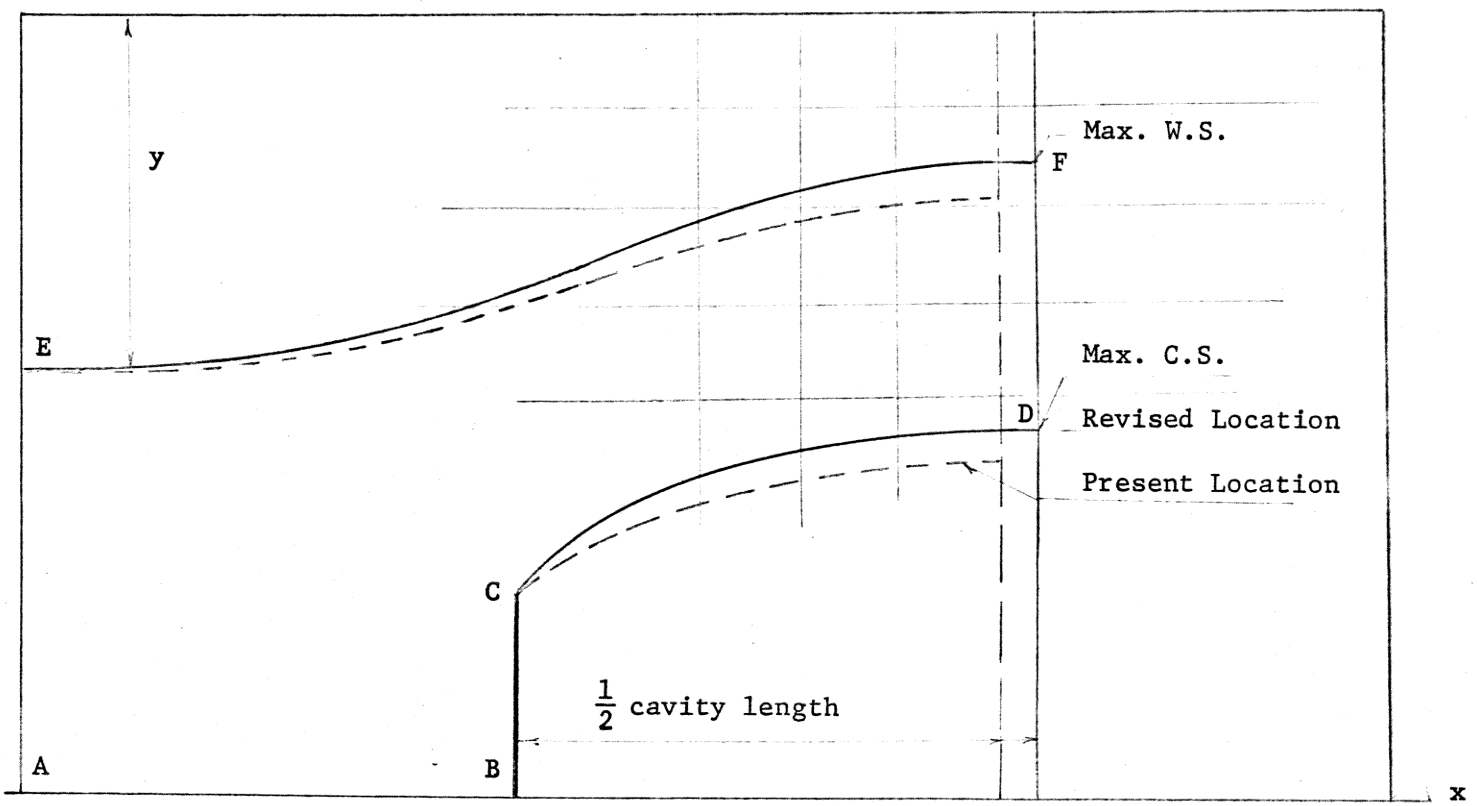

Figure 7c Riabouchinsky Model (Half Model)

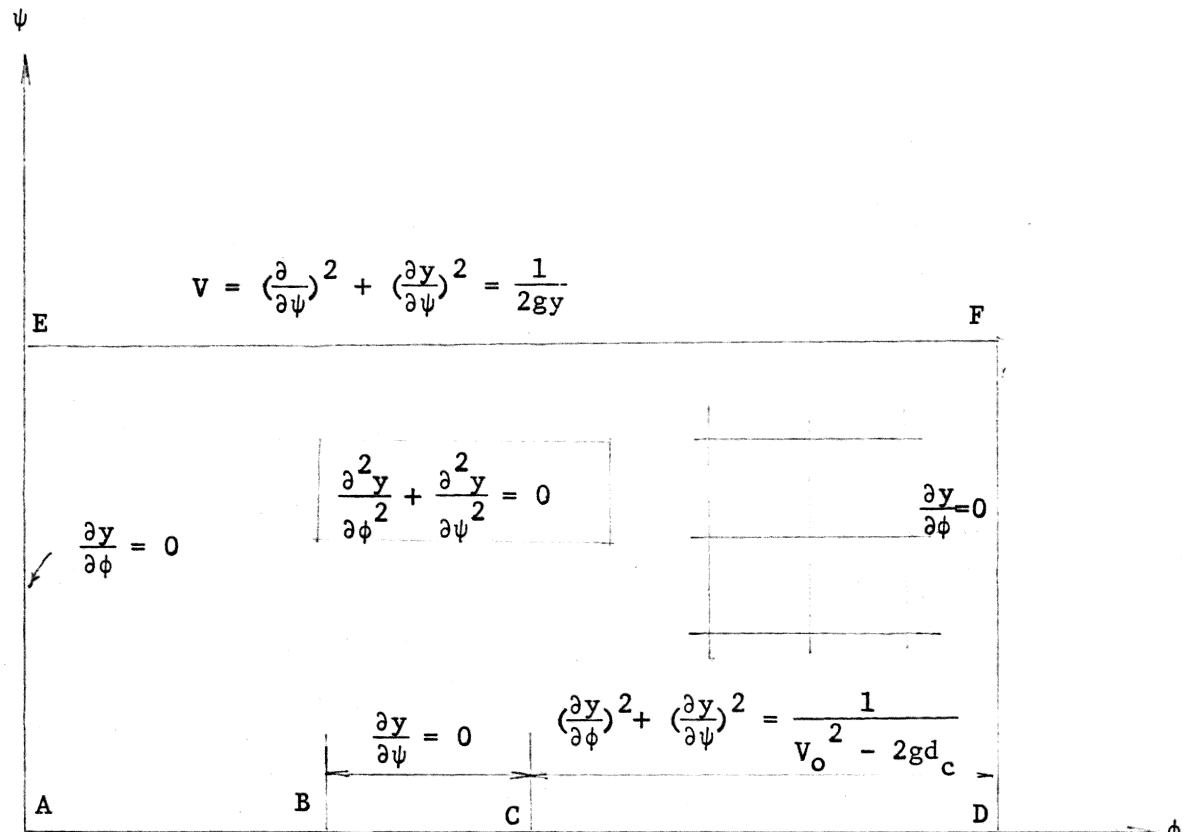

Figure 7d Transformed Plane (ϕ ~ ψ)

REFERENCES

1. Morris, Henry M. and Johns, J. Sterling, "Tumbling Flow in Open Channels". ASCE National Water Resources Meeting Preprint 1124.

2. Southwell, R. V. and Vaisey, G., "Relaxation Methods Applied to Engineering Problems. XII, Fluid Motions Characterized by 'Free' Stream-lines". Phil. Trans. Series A, Vol. 240, Nov. 1946, pp. 117-161.

3. Robertson, James M., "Hydrodynamics in Theory and Application". Prentice-Hall, Inc., Englewood Cliffs, N.J.

4. McNown, J. S., Hsu, E. Y. and Yih, C. S., 1955, "Application of the Relaxation Technique in Fluid Mechanics". Trans. Am. Soc. Civil Engineers, 120, 650-86. Proc. ASCE, July 1953.

5. Birkhoff, Garrett, "Calculation of Potential Flows with Free Streamlines". Journal of the Hydraulics Division, Proc. ASCE, Nov. 1961, pp. 17-22.

6. Garg, Satya P., "Calculation of Potential Flows with Free Streamlines". Journal of the Hydraulics Division, Proc. ASCE, July 1962, pp. 293-299.

7. Markland, E., "Calculation of Flow at a Free Overfall by Relaxation Method". Proc. Instn. Civ. Engrs. 1964.

8. Jeppson, R. W., "Techniques for Solving Free-Streamline, Cavity, Jet and Seepage Problems by Finite Differences" C.E. Dept. Tech. Rep. No. 68, Standford, Calif. Sept. 1966.

9. Mogel, Theodore R. and Street, Robert L., "A Numerical Method for Steady State Cavity Flows". Stanford University, Dept. of Civil Engineering, Feb. 1972.

10. Watters, Gary Z. and Street, Robert L., "Two-Dimensional Flow Over Sills in Open Channels". Journal of the Hydraulics Division, Proc. ASCE, July 1964, pp. 107-140.

11. Karki, Karam S., Chander, Subhash and Malhotra, Ramesh C., "Supercritical Flow Over Sills at Incipient Jump Conditions". Journal of the Hydraulics Division, Proc. ASCE, Oct. 1972, pp. 1753-1764.

REFERENCES (continued)

12. Carnahan, B., Luther, H. A. and Wilkes, James O., "Applied Numerical Methods". John Wiley and Sons, Inc., 1969.

13. Streeter, Victor L., "Handbook of Fluid Dynamics". McGraw-Hill Book Company, Inc., 1961.

14. Batchelor, G. K., "An Introduction to Fluid Dynamics". Chambridge at the University Press, 1967.

15. Durevich, M. J., "Theory of Jets in Ideal Fluids". Academic Press, New York and London, 1965.

16. Rand, W., "Flow Over a Vertical Sill in an Open Channel". Journal of the Hydraulics Division, Proc. ASCE, July 1965, pp. 97-121.

17. Narayanan, R. and Reynolds, Alan J., "Pressure Fluctuations in Reattaching Flow". Journal of the Hydraulics Division, Proc. ASCE, Nov. 1968, pp. 1383-1398.

18. McCorquodale, John A. and Giratalla, Mahmoud K., "Supercritical Flow Over Sills". Journal of the Hydraulics Division, Proc. ASCE, April 1972, pp. 667-677.

19. Wu, Th. Yao-Tsu, "Cavity and Wake Flows" from "Annual Review of Fluid Mechanics". 1972 Annual Reviews, Inc., California.

APPENDIX

COMPUTER FLOW DIAGRAM

The computer program is written in IBM FORTRAN language and has been run on the Burrough 6700 computer. It consists of a main program and four subroutines, COEF, CAVITY, SURFAC, and SABD. The main variables used in the program are described below:

Program Symbol	Definition
(Main)	
DEL	Number of subdivisions to be made in an original grid.
DC(J)	Percentage error measured for a boundary point on cavity surface at jth column.
DF(J)	Percentage error measured for a boundary point on free surface at jth column.
EH	Element height.
F	Froude Number.
HO	Total head.
II	Iteration counter for adjustment of free boundaries.
IS	Row number at uppermost bound of sub-grid system.
K	Row number for free surface at uniform flow section.
KT	Row number at uppermost bound of main grid system.

LB	Column number at left edge of sub-grid system.
LF	Column number at right edge of sub-grid system.
LL	Column number at which element sited.
MOC	A counter indicating the total number of grid points on cavity surface, which satisfy the boundary conditions.
MOS	A counter indicating the total number of grid points on free surface, which satisfy the boundary conditions.
NT	Column number at right edge of main grid system.
P	Pressure within cavity.
R(I,J)	Value of Residue at i, jth point.
SAL	Increment of ψ value.
S(I,J)	Value of ψ at i, jth point.
VB(J)	Velocity along cavity surface at jth column.
VS(J)	Velocity along free surface at jth column.
X(J)	Coordinate of a grid point along X-axis.
XX	Increment of grid spacing.
Y(I,J)	Coordinate of a grid point along Y-axis.
YB(J)	Location of a point on free surface at jth column.
YS(J)	Location of a point on free surface at jth column.

(Subroutine COEF)

$C_1(I,J)$	Distribution factor for left string at i, jth point.
$C_2(I,J)$	Distribution factor for right string at i, jth point.
$C_3(I,J)$	Distribution factor for lower string at i, jth point.
$C_4(I,J)$	Distribution factor for upper string at i, jth point.
ITM	Iteration counter for relaxation process.
SA	Allowable error for residue.

(Subroutines CAVITY and SURFAC)

AA	Amount of adjustment to be made on location of free boundaries.
DE(J)	Error measured for a point on cavity surface at jth column.
SS(J)	Error measured for a point on free surface at jth column.
TMAX	Max. error measured at free boundaries.

(Subroutine SABD)

IP	Row number at upper most bound of sub-grid system equivalent to IS in original grid system.
IN	Column number at right edge of sub-grid system equivalent to LB in original grid system.
ITT	Iteration counter for relaxation process in sub-grid system.
SFF	Increment of ψ value in sub-grid system.
XA	Increment of grid spacing in sub-grid system.

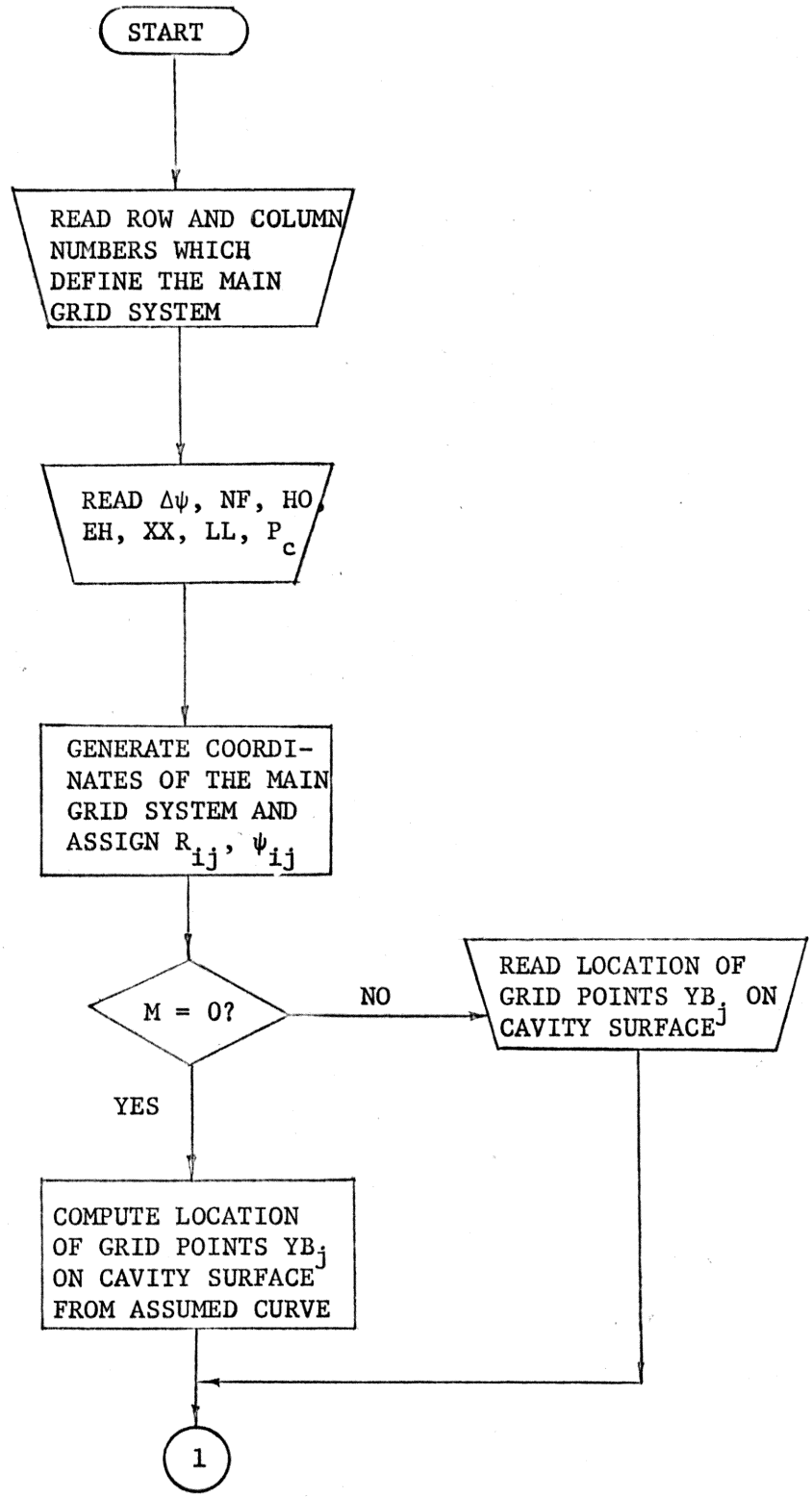
START
READ ROW AND COLUMN NUMBERS WHICH DEFINE THE MAIN GRID SYSTEM
READ $\Delta\psi$, NF, HO, EH, XX, LL, P_c
GENERATE COORDINATES OF THE MAIN GRID SYSTEM AND ASSIGN R_{ij}, ψ_{ij}
M = 0?
NO
READ LOCATION OF GRID POINTS YB_j ON CAVITY SURFACE
YES
COMPUTE LOCATION OF GRID POINTS YB_j ON CAVITY SURFACE FROM ASSUMED CURVE
1

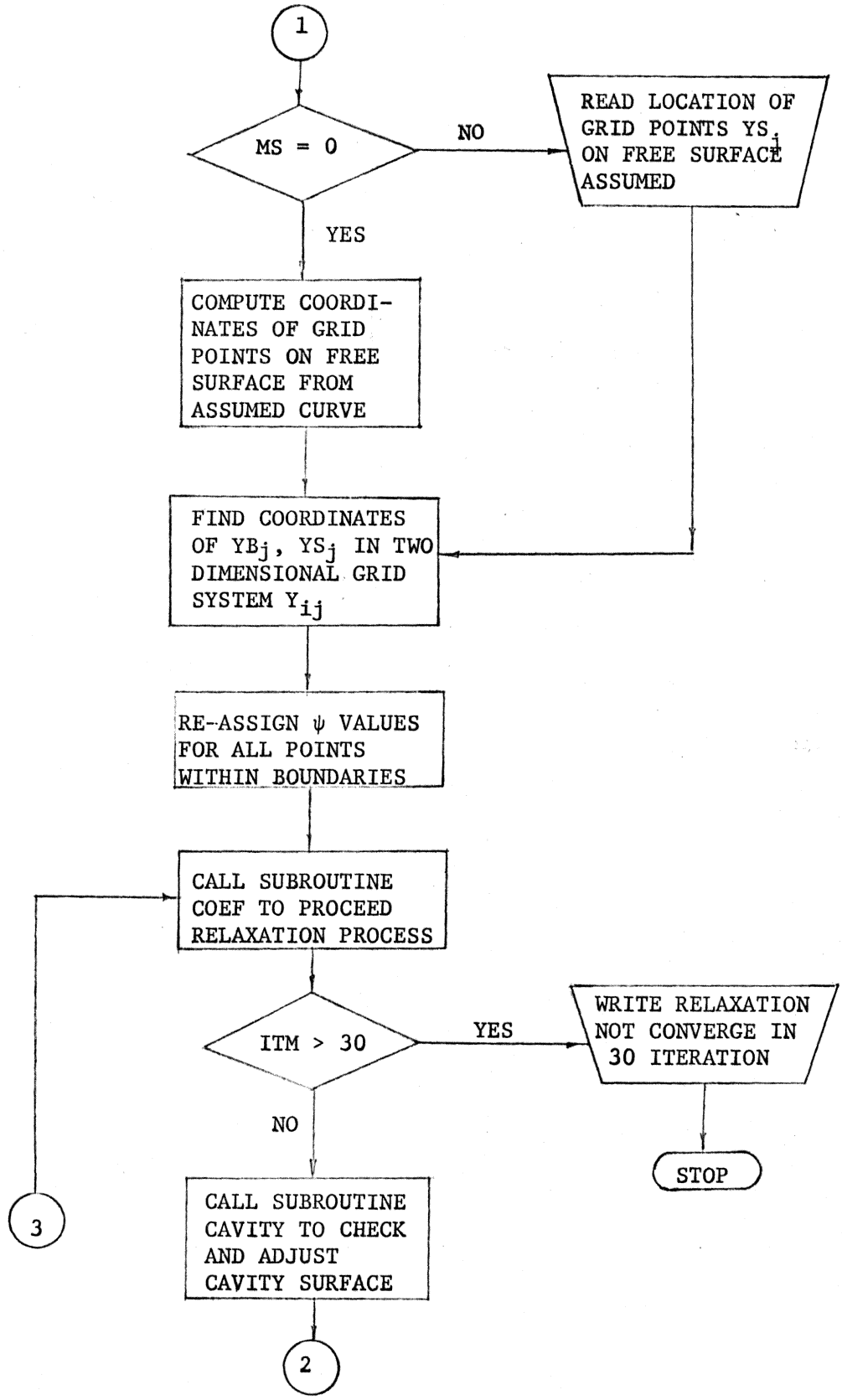
1
MS = 0
NO
READ LOCATION OF GRID POINTS YS$_j$ ON FREE SURFACE ASSUMED
YES
COMPUTE COORDINATES OF GRID POINTS ON FREE SURFACE FROM ASSUMED CURVE
FIND COORDINATES OF YB$_j$, YS$_j$ IN TWO DIMENSIONAL GRID SYSTEM Y$_{ij}$
RE-ASSIGN ψ VALUES FOR ALL POINTS WITHIN BOUNDARIES
CALL SUBROUTINE COEF TO PROCEED RELAXATION PROCESS
ITM > 30
YES
WRITE RELAXATION NOT CONVERGE IN 30 ITERATION
STOP
NO
CALL SUBROUTINE CAVITY TO CHECK AND ADJUST CAVITY SURFACE
3
2

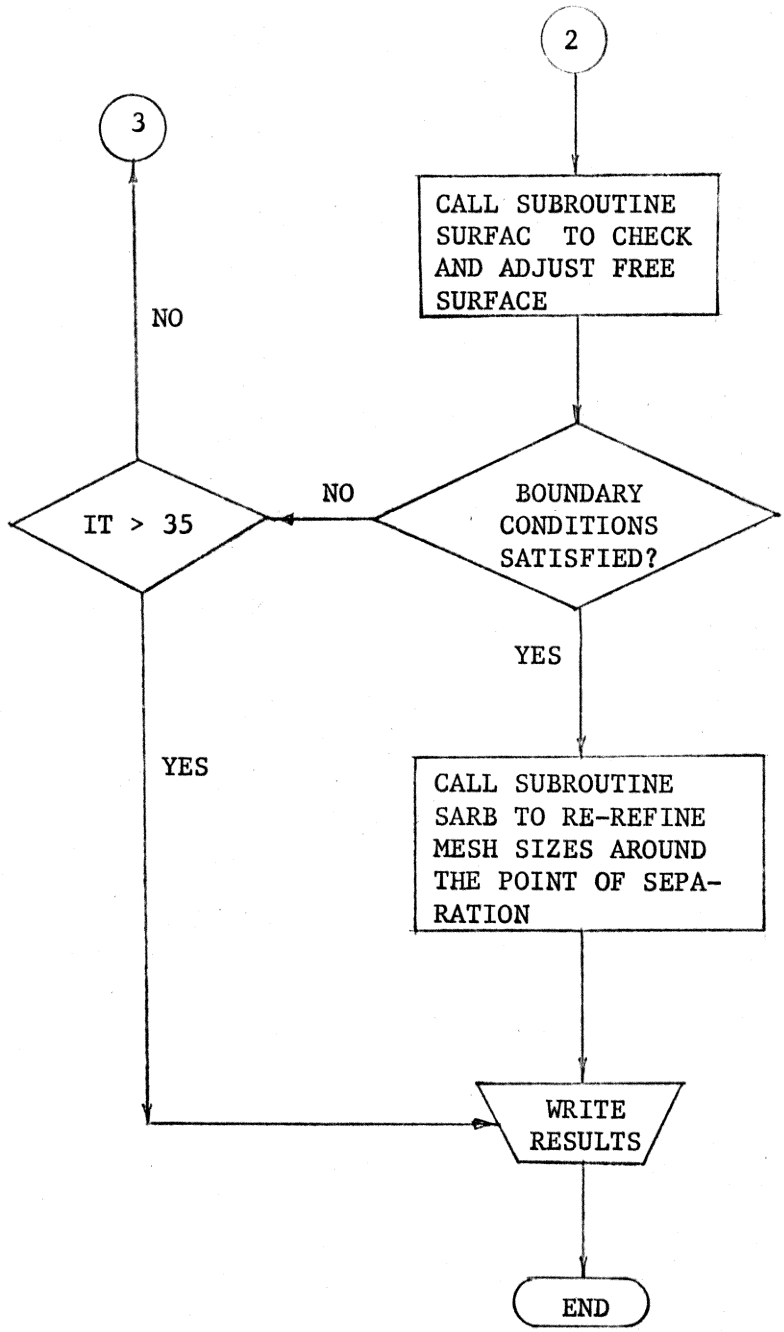
2
3
CALL SUBROUTINE SURFAC TO CHECK AND ADJUST FREE SURFACE
NO
BOUNDARY CONDITIONS SATISFIED?
NO
IT > 35
YES
YES
CALL SUBROUTINE SARB TO RE-REFINE MESH SIZES AROUND THE POINT OF SEPA-RATION
WRITE RESULTS
END

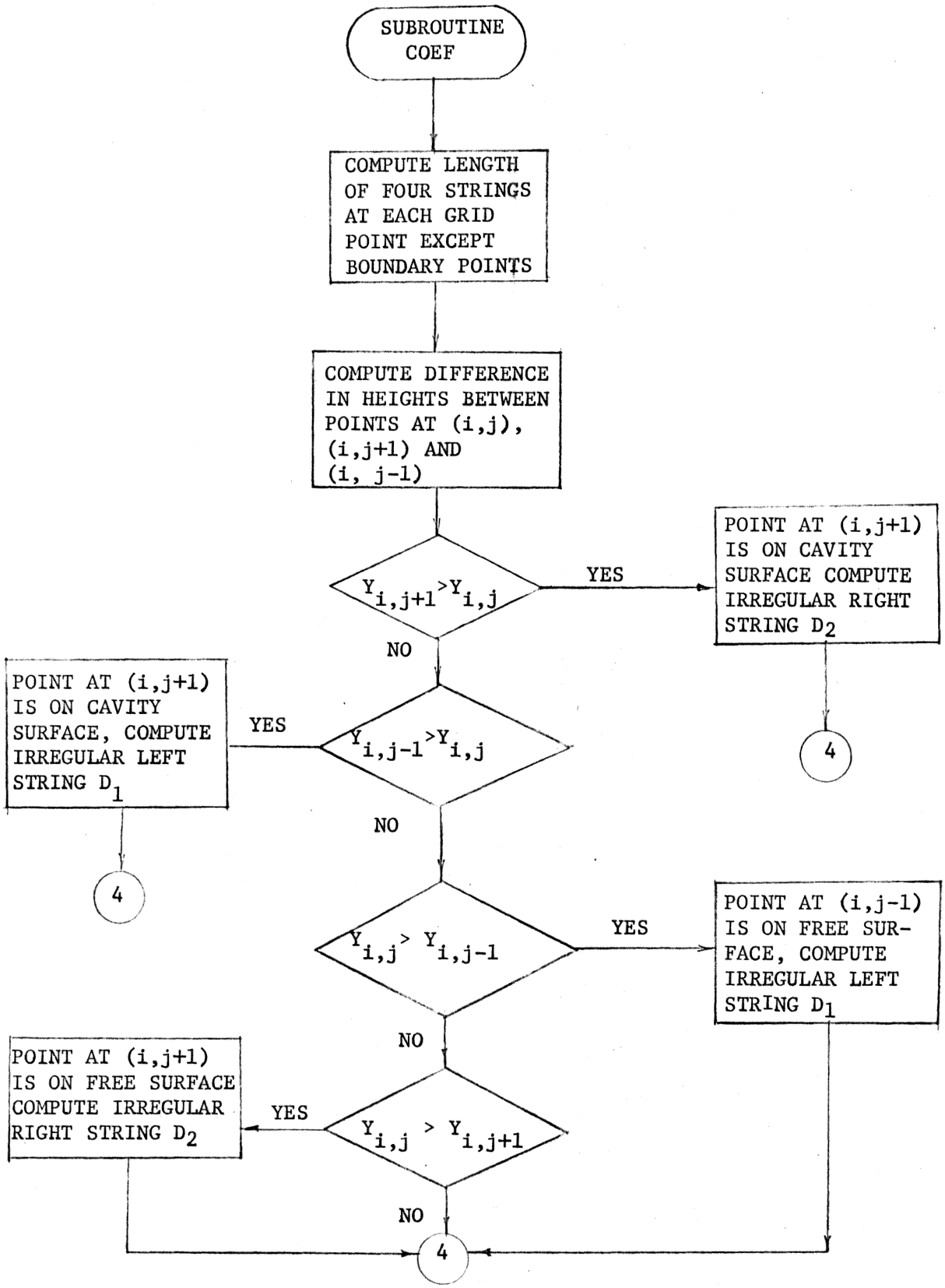
SUBROUTINE COEF
COMPUTE LENGTH OF FOUR STRINGS AT EACH GRID POINT EXCEPT BOUNDARY POINTS
COMPUTE DIFFERENCE IN HEIGHTS BETWEEN POINTS AT (i,j), (i,j+1) AND (i, j-1)
$Y_{i,j+1} > Y_{i,j}$
YES
POINT AT (i,j+1) IS ON CAVITY SURFACE COMPUTE IRREGULAR RIGHT STRING D_2
4
NO
$Y_{i,j-1} > Y_{i,j}$
YES
POINT AT (i,j+1) IS ON CAVITY SURFACE, COMPUTE IRREGULAR LEFT STRING D_1
4
NO
$Y_{i,j} > Y_{i,j-1}$
YES
POINT AT (i,j-1) IS ON FREE SURFACE, COMPUTE IRREGULAR LEFT STRING D_1
NO
$Y_{i,j} > Y_{i,j+1}$
YES
POINT AT (i,j+1) IS ON FREE SURFACE COMPUTE IRREGULAR RIGHT STRING D_2
NO
4

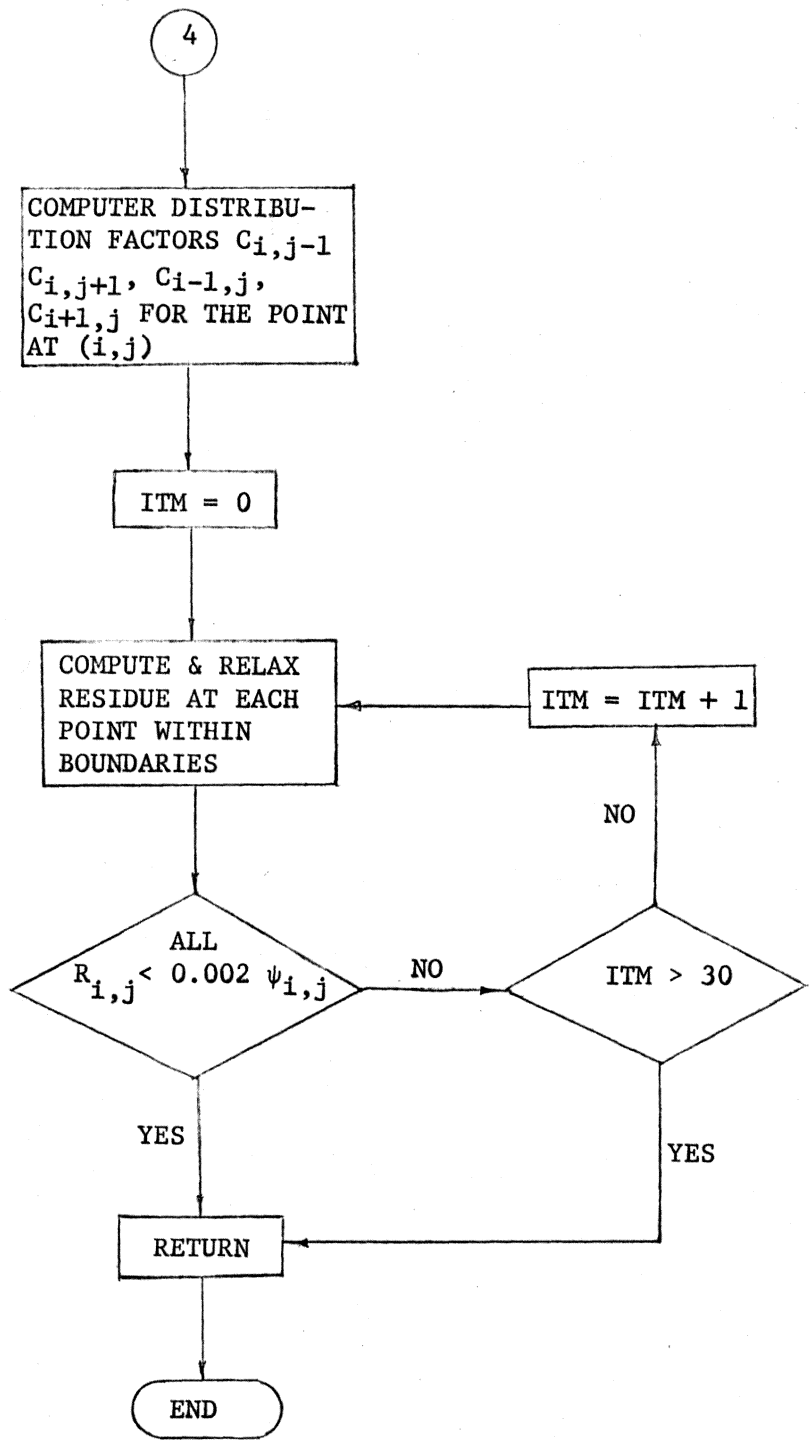
4
COMPUTER DISTRIBUTION FACTORS $C_{i,j-1}$ $C_{i,j+1}$, $C_{i-1,j}$, $C_{i+1,j}$ FOR THE POINT AT (i,j)
ITM = 0
COMPUTE & RELAX RESIDUE AT EACH POINT WITHIN BOUNDARIES
ITM = ITM + 1
NO
ALL $R_{i,j} < 0.002\ \psi_{i,j}$
NO
ITM > 30
YES
YES
RETURN
END

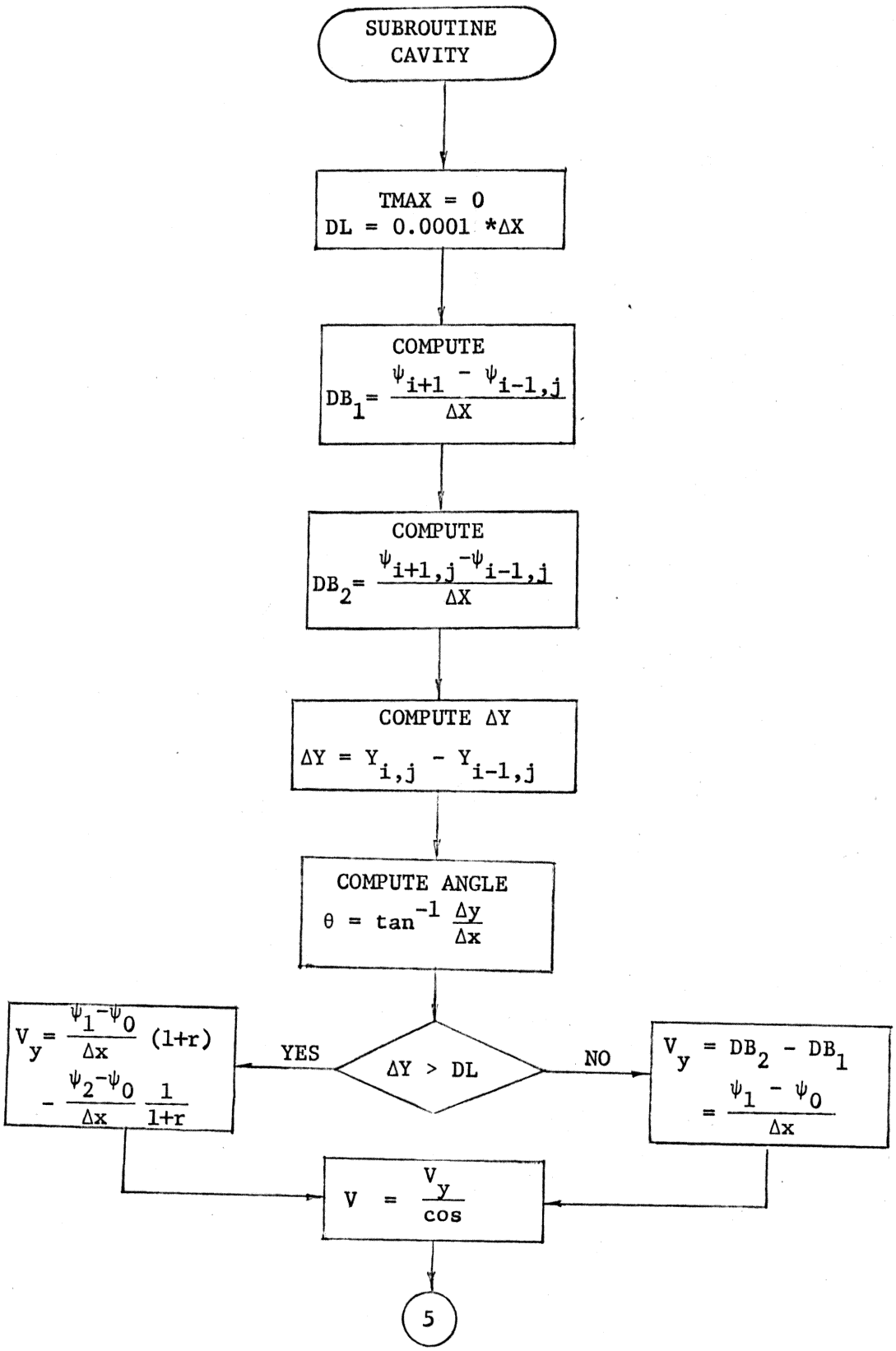
SUBROUTINE CAVITY
TMAX = 0
DL = 0.0001 *ΔX
COMPUTE
$DB_1 = \frac{\psi_{i+1} - \psi_{i-1,j}}{\Delta X}$
COMPUTE
$DB_2 = \frac{\psi_{i+1,j} - \psi_{i-1,j}}{\Delta X}$
COMPUTE ΔY
$\Delta Y = Y_{i,j} - Y_{i-1,j}$
COMPUTE ANGLE
$\theta = \tan^{-1} \frac{\Delta y}{\Delta x}$
ΔY > DL
YES
$V_y = \frac{\psi_1 - \psi_0}{\Delta x}(1+r) - \frac{\psi_2 - \psi_0}{\Delta x}\frac{1}{1+r}$
NO
$V_y = DB_2 - DB_1 = \frac{\psi_1 - \psi_0}{\Delta x}$
$V = \frac{V_y}{\cos}$
5

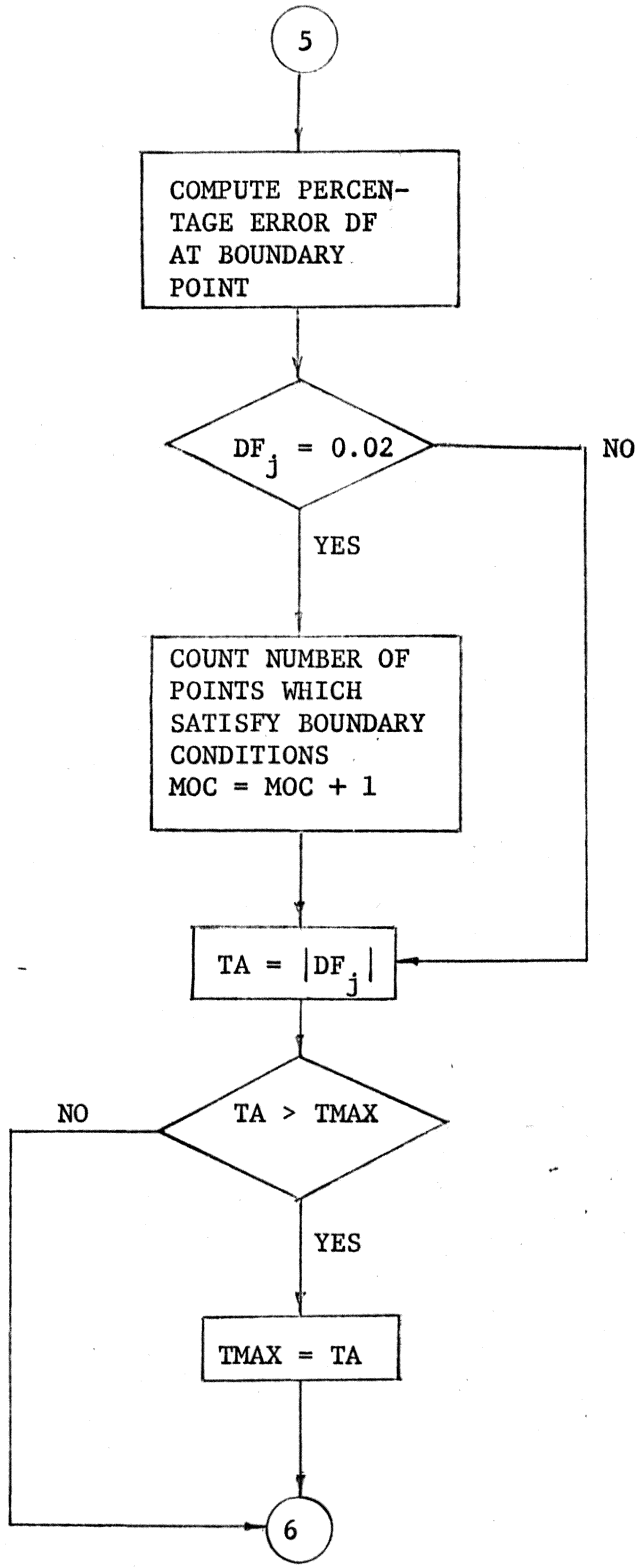
5
COMPUTE PERCEN-
TAGE ERROR DF
AT BOUNDARY
POINT
DF_j = 0.02
NO
YES
COUNT NUMBER OF
POINTS WHICH
SATISFY BOUNDARY
CONDITIONS
MOC = MOC + 1
TA = |DF_j|
NO
TA > TMAX
YES
TMAX = TA
6

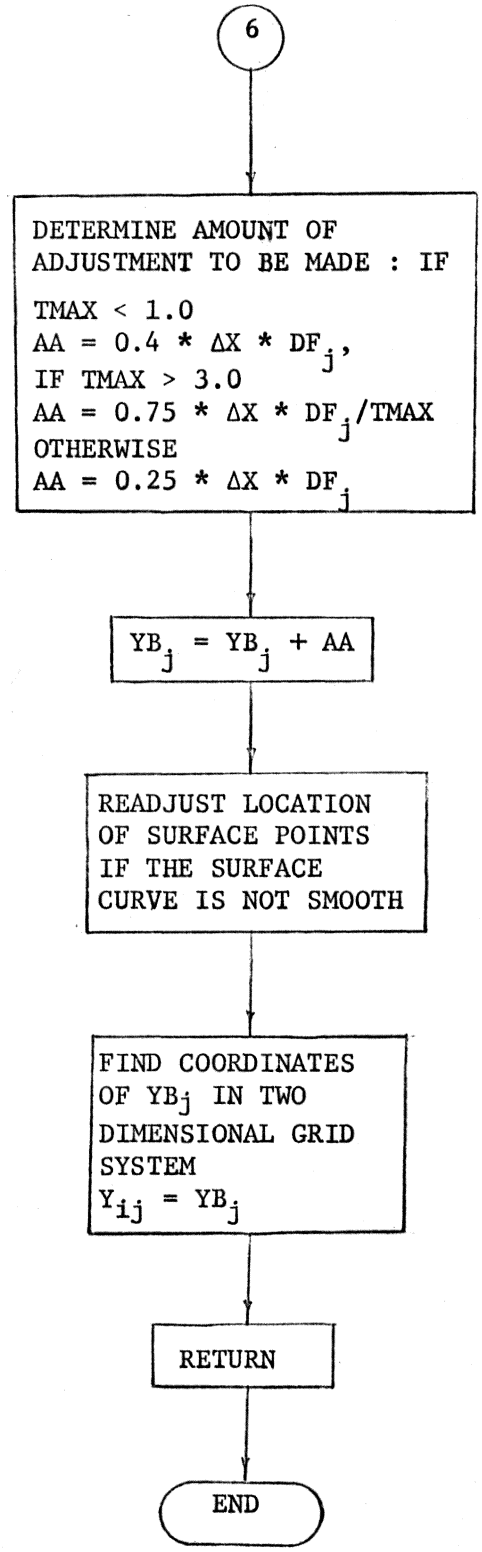
6
DETERMINE AMOUNT OF ADJUSTMENT TO BE MADE : IF
TMAX < 1.0
AA = 0.4 * ΔX * DF_j,
IF TMAX > 3.0
AA = 0.75 * ΔX * DF_j/TMAX
OTHERWISE
AA = 0.25 * ΔX * DF_j
YB_j = YB_j + AA
READJUST LOCATION OF SURFACE POINTS IF THE SURFACE CURVE IS NOT SMOOTH
FIND COORDINATES OF YB_j IN TWO DIMENSIONAL GRID SYSTEM
Y_ij = YB_j
RETURN
END

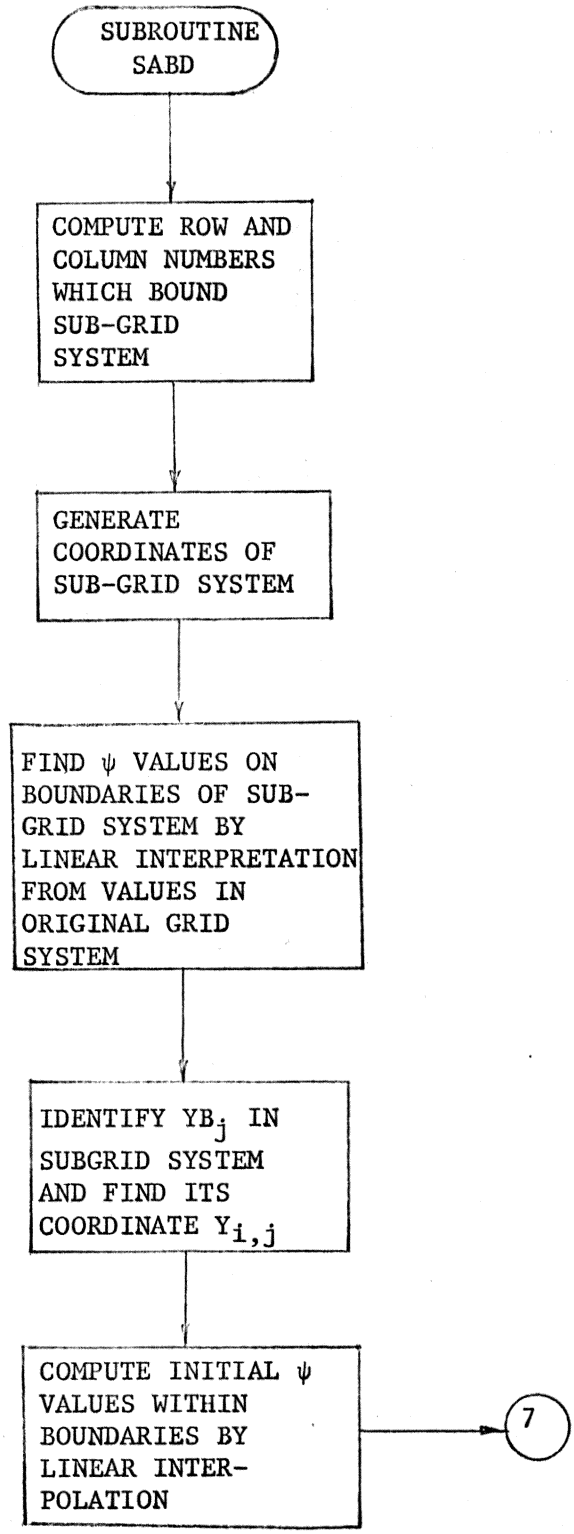
SUBROUTINE SABD
COMPUTE ROW AND COLUMN NUMBERS WHICH BOUND SUB-GRID SYSTEM
GENERATE COORDINATES OF SUB-GRID SYSTEM
FIND ψ VALUES ON BOUNDARIES OF SUB-GRID SYSTEM BY LINEAR INTERPRETATION FROM VALUES IN ORIGINAL GRID SYSTEM
IDENTIFY YB_j IN SUBGRID SYSTEM AND FIND ITS COORDINATE $Y_{i,j}$
COMPUTE INITIAL ψ VALUES WITHIN BOUNDARIES BY LINEAR INTER-POLATION
7

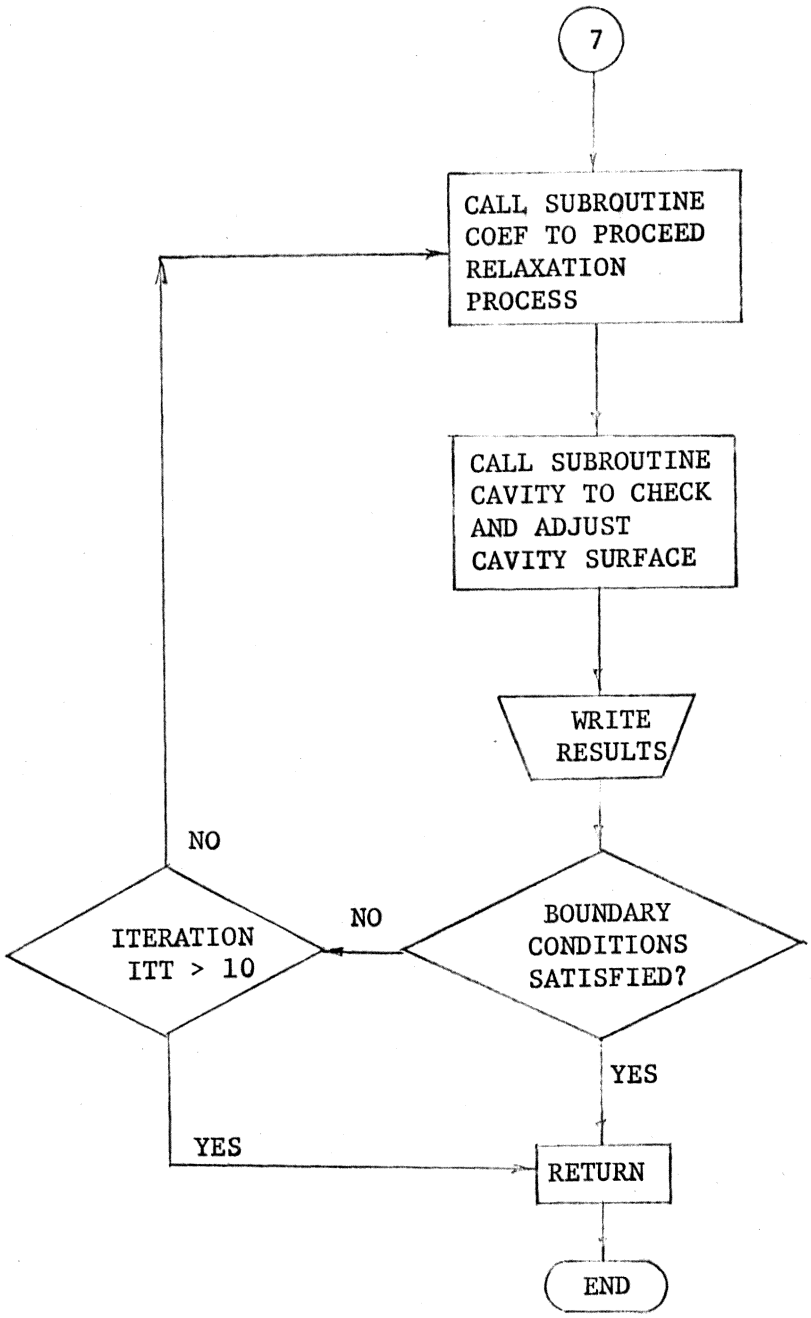

NOTE: THE FLOW CHART FOR SUBROUTINE SURFAC IS THE SAME AS THAT OF SUBROUTINE CAVITY. THEREFORE IT WOULD NOT BE REPEATED HERE.

The vita has been removed from the scanned document

CAVITY FLOW PAST AN OBSTACLE INCLUDING GRAVITY EFFECTS

by

Chao-yung Ou

(ABSTRACT)

The object of this study was to use the relaxation method to find the solution of cavity flow past a two-dimensional roughness element in an open channel with gravity effect included. The method developed is based on an inviscid, irrotational and incompressible flowfield, using a finite-difference representation with stream functions as dependent variables. A computer program is developed to adjust free boundaries systematically and to facilitate numerical computation. The Helmholtz-Kirchhoff cavity model is used in this study, with sixteen primary cases analyzed. The computer results are plotted and the computer listing is given. From the results, it is found that the Helmholtz-Kirchhoff model is not applicable because no finite length of cavity can be obtained. Finally, the use of the Riabouchinsky model is recommended.